A NOVEL METHOD TO INTEGRATE INTRA-ORAL SCAN MODELS WITH 3D FACIAL IMAGES

by

Amanda Justine Sigouin

BSc., Simon Fraser University, 2013

DMD, The University of British Columbia, 2017

A THESIS SUBMITTED IN PARTIAL FULFILLMENT OF

THE REQUIREMENTS FOR THE DEGREE OF

MASTER OF SCIENCE

in

THE FACULTY OF GRADUATE AND POSTDOCTORAL STUDIES

(Craniofacial Science)

THE UNIVERSITY OF BRITISH COLUMBIA

(Vancouver)

March 2023

The following individuals certify that they have read, and recommend to the Faculty of Graduate and Postdoctoral Studies for acceptance, the thesis entitled:

A Novel Method for Integrating Intra-Oral Scan Models with 3D Facial Images

submitted by Amanda Justine Sigouin in partial fulfillment of the requirements for

the degree of Master of Science

in Craniofacial Science

Examining Committee:

Dr. Bingshuang Zou, Associate Professor, Division of Orthodontics, UBC
Supervisor

Dr. Jolanta Aleksejuniene, Associate Professor, Director of Graduate Studies, UBC
Supervisory Committee Member

Dr. Vincent Lee, Assistant Professor of Teaching, Division of Prosthodontics, UBC
Supervisory Committee Member

Dr. David MacDonald, Professor, Chair, Oral & Maxillofacial Radiology, UBC
Additional Examiner

Abstract

Objectives: Three-dimensional (3D) imaging is becoming more mainstream with advances in digital technology and reduction in cost. Two-dimensional (2D) imaging has been the standard in orthodontics but it would be beneficial to examine virtual 3D patients for diagnosis, treatment planning, and assessment of growth and treatment outcomes with no use of ionizing radiation. This study aimed to validate the Bellus Arc7 3D facial scanner and test a novel method for integrating intraoral scans with 3D facial images to create a virtual patient.

Methods: Part I entailed validation of Bellus Arc7 using the conventional reference standard, the 3dMDface system. Three subjects were selected, and for each 4 images were taken on two occasions one week apart. Images were uploaded, superimposed, and a 3D heat map was generated for comparison using Geomagic Control X processing software. Part II compared a novel merging technique from 14 participants recruited from UBC Graduate Orthodontic Program. For each subject, 5 images were captured (two images using Trios intraoral scanner, one facial scan with Bellus Arc7, and two with Artec Space Spider). The intra-oral scan of the upper dentition and the Arc7 3D facial scans were merged via the transferring of the perioral scan to develop a virtual patient. The reference 3D virtual image from the alignment of the dental scan and Artec Space Spider facial scans was used for comparison. The surface-to-surface root mean square and point-to-point deviation values between the two meshes were analysed.

Results: Part I showed the root mean square for Bellus Arc7 as compared to the reference 3dMD to be 1.16 ± 0.41 mm for all three subjects, which is clinically acceptable for soft tissue measurements. Part II showed that relative to the merged Artec Space Spider scans, the root mean square difference of the merged Arc7 scans was 1.52 ± 0.54 mm. For the point-to-point deviations in the dentition there was a relatively wide range of mean differences.

Conclusions: The results indicated that creating a 3D patient by merging the dental scan with 3D facial images acquired with Bellus Arc7 is adequate quality for most clinical applications, albeit very technique sensitive.

Lay Summary

In the field of orthodontics, two-dimensional (2D) images such as photographs and radiographs, as well as dental casts have been used along with a clinical examination for diagnosis, treatment planning, patient education and assessment of treatment outcome. With the advances in digital technology and a reduction in cost, three-dimensional (3D) images are becoming more mainstream technology. The benefits of having a non-invasive method to generate a virtual 3D patient would be beneficial to both clinicians and their patient.

This study first validated the Bellus Arc7 facial scanner against an already authenticated facial camera, the 3dMD face system. Next, we tested a novel method of integrating intra-oral scan models with 3D facial scans to generate a 3D patient.

Preface

Dr. Bingshuang Zou suggested the idea for the research topic as a continuation of a previous graduate student, Dr. James Andrews, master's thesis project. The research sample was gathered from the UBC Faculty of Dentistry patients, residents, and staff members. The methodology was discussed and revised by committee members Drs. Bingshuang Zou, Jolanta Aleksejuniene and Vincent Lee. Data collection, entry and analyses were performed by Dr. Amanda Sigouin and assisted by Drs. Scott Panther and Jeremy Ho in the initial protocol testing period.

This study was approved by the University of British Columbia Office of Research Services, Institutional Research Board (Certificate number: H21-00949).

Table of Contents

List of Tables

List of Figures

List of Abbreviations

CBCT: Cone Beam Computed Tomography

DICOM: Digital Imaging and Communications in Medicine

FS: Facial Scan

FOV: Field of View

IOS: Intraoral Scan

LS: Laser Scanner

MRI: Magnetic Resonance Imaging

OBJ: Object File

RMS: Root Mean Square

STL: Standard Triangle Language

SP: Stereophotogrammetry

SLS: Structured Light Scanner

2D: Two-Dimensional

3D: Three-Dimensional

Acknowledgements

I offer my sincere appreciation to my co-residents, the faculty, and the staff at UBC Graduate Orthodontics. It has been a pleasure working, learning, and sharing in this journey with you for the last three years.

I owe particular thanks to Dr. Bingshuang Zou for sharing her wealth of knowledge and offering her unwavering encouragement and support in clinic and as my research supervisor. Thank you to my research committee members Dr. Jolanta Aleksejuniene and Dr. Vincent Lee for their time, guidance, and support during my master's project.

An extra special thank you goes out to my parents, my brother, and my husband for loving me unconditionally and being there to support me as I ventured back to post-secondary school for a third time. I am truly blessed to have you all in my life.

Dedication

I dedicate my thesis to my incredible family. My husband Devin, my parents Lorri and Jim and my brother Nicolas. Thank you for always believing in me even when I had doubts in myself and for providing me with the courage I needed to achieve my dreams.

Chapter 1: Introduction

1.1 History of Orthodontic Records

In orthodontics and orthognathic surgery, there are three key tissue groups to consider; facial soft tissue (skin, connective tissues, fat and muscles), facial skeleton (bone and cartilage) and dentition, which can be referred to as the triad [1]. The triad plays a key role in diagnosis and planning orthodontic treatment and orthognathic surgery. All three tissue groups require a detailed assessment to provide the patient with the best functional, esthetic, and successful long-term outcome.

In 1897, Babcock introduced the use of plaster casts for model surgery, and this became the 'gold standard' for planning postoperative occlusion. Then, in 1931, Broadbent claimed that cephalograms were more accurate for treatment planning since they displayed the relationship between the facial skeleton and dentition. This strategy provided the patient with a good functional outcome but sometimes with a poor esthetic result due to the lack of consideration of all three components of the triad [1], [2]. Later, digital photography was introduced to assess facial harmony. This provided the clinician with a more proportional focus on the three structures of the triad but due to the two-dimensional nature, it did not address the volumetric changes of all the facial portions, especially in asymmetrical cases [1].

Conventionally in orthodontics, study models, two-dimensional (2D) photographs and 2D radiographs (panoramic, and lateral cephalometry) have been used for diagnosis and treatment planning. However, there are limitations with the use of 2D imaging systems including exposure to radiation, radiographic projection error and inaccuracies in radiographic measurements and identification of three-dimensional (3D) structures from 2D images [3].

Since 1922, 3D photography, which combines several images of a subject taken from different angles into one 3D topography, has been available in the field of dentistry. The use of this technology initially was not advantageous in an orthodontic setting due to technical limitations, low image resolution, and high cost of purchase and computer software programs [4].

While Cone-beam computed tomography (CBCT) imaging technology provides an accurate representation of the 3D shape and position of the jaws it has its limitations including higher radiation exposure compared to 2D radiographs. In addition, patients who have metallic dental restorations and/or orthodontic brackets can present with streaking artifacts on the image, which can impede the accurate identification of potentially critical areas. Superimposition of CBCT images with digital dental models can alleviate the effects caused by undesired artifacts and provide an accurate interocclusal relationship of the teeth, which is crucial for treatment planning for orthognathic surgery [5].

In orthodontic patients who do not require CBCT imaging, having a virtual 3D model for diagnosis, treatment planning, patient education and assessment of growth and/or treatment outcomes would be beneficial for the clinicians and their patients. With the advancements in digital technology and reduction in cost, 3D imaging including laser scanning and (3D) photogrammetry are becoming more mainstream technology.

1.2 3D Facial Scanners

3D photography is a non-invasive method to acquire a 3D representation of the craniofacial complex. The 3D reconstruction not only provides linear measurements, but it can

also calculate surface distances, surface areas and volumes. This provides a more comprehensive and in-depth assessment of the patient's craniofacial morphology compared to traditional methods [2], [6], [7].

There are various 3D scanning technologies on the market today, each with advantages and disadvantages. The various scanner types depend on different physical principles. Laser 3D scanning technology uses a laser line or single laser point to scan across an object [8], [9]. The main advantages of laser scanners, besides producing accurate 3D facial models, is that they are relatively inexpensive and easy to handle. The main disadvantage of laser scanning is the longer capture time, thus it is inconvenient to use it in pediatric cases [7]. Structured light scanners (SLSs) use trigonometric triangulation by projecting visible or infrared light on the surface of an object/face and inferring the 3D shape based on the distortion of the projected pattern [8], [9]. Stationary SLSs allow for rapid image capture and with regards to facial assessment demonstrated high accuracy and precision but in comparison to stereophotogrammetry, they often lack complete surface coverage. The introduction of portable and handheld SLSs was developed to overcome this limitation [10]. Stereophotogrammetry systems construct a 3D image from 2D photographs taken by two or more cameras at different angles. [8], [9]. The main advantage is the short acquisition time and simple utilization. Thus, making it a great choice for soft tissue capture in pediatric patients specifically those infants with craniofacial deformities, for example, cleft lip and/or palate patients. While stereophotogrammetry is very efficient in capturing facial morphology, it struggles to capture areas with tissue reflection, hair, and curved surfaces such as ears, eyes, and teeth [3], [7], [11]. In addition, these systems are often not practical for use in most clinical settings given their large size, lack of portability, complex setup, need for calibration and high cost [10]. Another system for capturing 3D data is volumetric

methods, these compute 3D shapes from 2D slices, for example, computer tomography (CT) or magnetic resonance imaging (MRI) [9].

Another way to categorize 3D scanning technology is based on the type of equipment of the optical device, namely stationary or portable/handheld systems. Stationary systems have the advantage of being stable, which allows faster image capture, and thus reduces the effect of any motion artifacts. Handheld scanners have the benefit of being highly portable, however, involuntary facial movements of the subject can be magnified due to the prolonged scanning time and unstable movements of the scanner [8].

Table 1.1: Imaging Systems Technical Overview

3D Imaging Technology	3dMD face System *reference Part I	Bellus Arc7 Camera	Artec 3D Space Spider Handheld *reference Part II	Trios 3Shape IntraOral Scanner
Imaging Modality	Stereophotogrammetry	Structured Light (infra-red)	Structured Light (blue)	Structured Light
Capture Time	~1.5 ms at highest resolution	3 secs	60-180 secs	360- 600 secs
3D point Accuracy*	0.2 mm	0.4mm	0.05mm	0.01 mm
Output files	Textured mesh/ point cloud	Textured mesh/ point cloud	Textured mesh/ point cloud	STL output
Ease of use	Requires continuous calibration	Simple calibration	Calibration required	Calibration required
Accessibility	Stationary	Portable to an extent	Easily portable	Portable to an extent
Cost	$84,000	$5,800 +	$25,000	>$20,000

* 3D point Accuracy as stated by the manufacturer

1.2.1 Merging Methods

Even with the advances in 3D technology, none of the craniofacial imaging techniques can capture the complete triad with optimal quality. This can only, currently, be achieved by 'image fusion' employing different imaging techniques to create a 3D virtual patient that can display all the triad elements [1], [12]. An image fusion model is defined as a composition of at least two imaging techniques [1]. The creation of a 3D virtual patient is dependent upon the integration of different file types (e.g. DICOM, STL, OBJ) and the probability of fusion into a replicable model. 3D data can be merged using three fusion methods; point-based, surface-based and voxel-based [12], [13]. The point-based method depends on matching corresponding landmarks, usually a minimum of three manually selected anatomic points, while the use of congruent surfaces or voxels depends on manually selecting regions [13], [14]. According to Wampfler and Gkantidis, 2022 [14], surface-based registrations perform superiorly to landmark-based registration. Overall, larger reference areas are preferred to smaller areas as they are less prone to operator or artifact-related errors, however, using larger regions does lead to including areas that may change over time [14]. A 2020 systematic review found that the surface-based registration method was most frequently used for 3D object superimposition, followed by the point-based method with or without fiducial markers [15]. The absence of clear markers on the skin can lead to inaccuracies in the scanned data when scanning a large area without distinct markers [8], [16].

It is vital to independently validate new imaging technology, and assess the accuracy and precision of the scanners, as well as the merging method. In anthropometric studies, accuracy consists of trueness and precision [17]. Trueness is defined as the agreement between a specified measurement and its "true value" and precision is defined as the ability of a specific

measurement to be consistently reproduced. Precision can be considered equivalent to reliability in this context.

Many different techniques have been described in the literature for merging imaging data [12], [13], [16], [18], [19]. As mentioned above, although stereophotogrammetry is accurate for capturing the external soft tissue, it struggles to accurately capture the dentition and gingiva due to their shiny surface, which affects how the computer constructs that region [18]. This may not be a concern in the field of plastic surgery but is a limitation of many 3D scanners for use in the field of prosthodontics and orthodontics. Rangel *et al.* [18] in 2008 proposed a method to integrate a patient's digital dental casts into a 3D facial image. They used four corresponding points, maxillary and mandibular central and lateral incisors for superimposition of the digital dental cast and a digital 3D image and found the average distance was 0.35mm ± 0.32mm. Pérez-Giugovaz *et al.* [19] study in 2020 demonstrated a successful superimposition technique between facial and intraoral scans (IOS) using intraoral scan bodies, but this technique adds an additional step and cost due to the fabrication of the scanning body.

1.2.2 Stable Reference Area

Several of the studies described above first used dental landmarks or scanning bodies to merge the intraoral scan with a 3D facial scan of the patient smiling and then merged the 3D facial scan with lips at rest with the merged IOS and 3D scan using the forehead as a reference [1], [12], [13], [18]–[20].

In 2012, Jayaratne *et al.* [21] used colour maps to assess the accuracy of superimposition of CBCT and 3D photographs and their findings revealed that the forehead, root of the nose and zygoma were the most appropriate facial regions for 3D imaging registration. As well,

Zedníková Malá *et al.* [22] in 2018 examined the soft-tissue and skeletal facial profile curves from 86 lateral head cephalograms. Their findings demonstrated that the strongest association between skeletal contour and overlying soft tissue was exhibited by the region of the forehead, followed by the region of the nasal root and then the lower lip and chin.

Thus, we propose a proof-of-principle study to examine the feasibility of using the Trios 3Shape intraoral scanner to scan the forehead of the patient along with the maxillary teeth to merge with the 3D facial scan.

The purpose of this study is to evaluate the accuracy and precision of two different 3D facial scanners and test a novel method of merging the intraoral scan with the 3D facial scan using the forehead and bridge of nose as a reference.

Null Hypotheses:

#1: There is no difference in the accuracy of the two different 3D facial scanning systems.

#2: Using a perioral scan including the patient's forehead and the surface of maxillary anterior teeth for merging 3D facial scans with intraoral scans to create a virtual patient produces measurements with an error which is within clinically acceptable levels.

Chapter 2: Materials and Methods

The study was approved by the University of British Columbia Clinical Research Ethics Board (Certificate number: H21-00949).

2.1 Study Design

Part I of the study involved three subjects, one mannequin and two adults from the Faculty of Dentistry at the University of British Columbia. Part II of the study involved 14 human participants recruited from the UBC Graduate Orthodontics Program including both pre-orthodontics patients, residents, and staff. Of the 14 participants, there were 10 females and four males, and the age range was 10-54 years. Each subject signed a written informed consent to participate in the study. All jewelry was removed prior to imaging. Extraneous hair was also retracted off the face before scanning. Exclusion criteria included subjects with craniofacial deformations, pathologies, impairments, or traumatic events involving facial areas. Subjects with beards were also excluded from the study as excess facial hair can impact the image quality.

2.2 Data Collection

2.2.1 Part I

The craniofacial region of three subjects (two humans, and one mannequin) was captured using two different 3D imaging systems: the reference data, the 3dMDface system (3dMD, Atlanta, GA) and the measured data, Bellus Arc7 (Bellus3D, Campbell, CA, USA). For the two human subjects, two images were captured on each of the cameras, one repose and one smiling, and such images were repeated one week later. For the mannequin subject, only a repose image was captured on both cameras and then repeated one week later. The mannequin head was mounted

on a broom handle and secured to a tripod during image capture to eliminate motion artifacts (Figure 2.2). The same researcher gave each participant strict instructions during the scanning procedure, thereby enhancing data quality. Before capturing the smiling image participants were asked to produce a smile they could hold for a minimum of 10 seconds.

Subject imaging with both camera systems was undertaken in the Digital Imaging Lab at the University of British Colombia's Dental Faculty. The data collection ran over a period of two weeks. The 3dMDface system was calibrated at the beginning of each session in accordance with the manufacturer's instructions, which were as follows: (Figure 2.1)

1.) Activate the calibration procedure in the 3dMD acquisition software by clicking on the icon that looks like an upside down "T"
2.) With the mouse, hover the cursor over the icon that says, "Acquire 1st Image Set"
3.) Lift the mouse off the table and hold the mouse in your right hand, with the other hand take the calibration board and center yourself between the two modular units
4.) Hold up the calibration board, face the dots on the calibration board towards the cameras
5.) Lean the calibration board back towards you, approximately 30 degrees, centering the dots and match up the bold black horizontal lines on the board, with the bold red lines on the grid of the computer monitor (Ensure there are at least two dots on either end of the bold red horizontal line)
6.) Left click the mouse in your hand, which processes that image and brings up another screen to take the second image set. This time lean the calibration board forward, approximately 30 degrees, centering the dots the same as was done for the first image acquisition

7.) When you are satisfied with the position left click the mouse once again, which processes the image and now the image of the subject can be captured.

The Bellus Arc7 system was calibrated when the camera was initially set-up and was recalibrated if poor scanning results occurred or the investigator was not able to get the red oval to turn green during the subject scanning. Calibration is initiated under the settings side bar. Upon clicking the calibration tab this provides the user with a list of instructions on the screen to recalibrate the cameras.

Each subject was positioned at a fixed distance from the 3dMDface camera (as per camera manufacturer-specific instructions), and the image was captured. Image capture is almost instantaneous at 1.5 milliseconds. The 3dMD consists of two modular units, each with six machine vision cameras and an industrial-grade flash system synchronized in a single capture. The system incorporates both active and passive structured lights in stereophotogrammetry. A random light pattern was projected onto the subject's face while the camera captured digital images and the software triangulates the captured images into a 3D image. 3D images were processed and generated by the 3dMD software. The software automatically incorporates information from all camera viewpoints per frame to generate a 3D point cloud so there is no manual stitching or registration required. Within the software, the images could be inspected to ensure complete capture of the desired regions/landmarks, as well as ensure absence of any acquisition errors. Imaging of the three subjects with the Bellus Arc7 camera(s) was carried out in the same room, with the same lighting conditions within 10 minutes of the initial 3dMD image capture. Each subject was positioned with their head in front of the center camera roughly 35 cm away. The software guides the subject on the correct head position as they line it up within an oval circle on the screen and the oval turns green when the head is the correct distance away from the center

camera. Subjects were instructed by the investigator to hold still during the 3-second capture time. Seven images are captured during each scan and can be viewed as individual images while the software stitches together the 3D model. After the scan processing was complete, prior to exporting, the image was inspected within the model viewer page to ensure complete capture of the desired regions/landmarks. When the researcher was satisfied with the scan, the image was saved in uniform triangulation, which generated the same number of triangles every time and was saved as an OBJ file.

All recorded data sets were stored securely on a UBC dentistry hard drive. Face surface scans in OBJ data files for each participant were uploaded for analysis into the Geomagic Control X (3D systems, Rock Hill, South Carolina, USA) software. Each participant's data were analyzed separately.

Figure 2.1: 3dMD Calibration Board Set-up

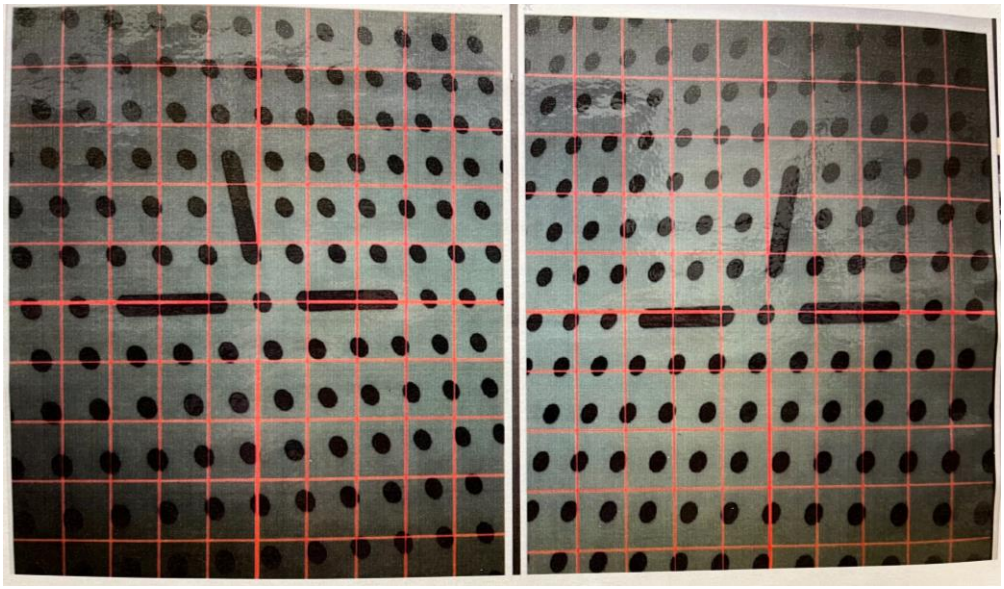

Figure 2.2: 3dMDFace System Camera Set-up

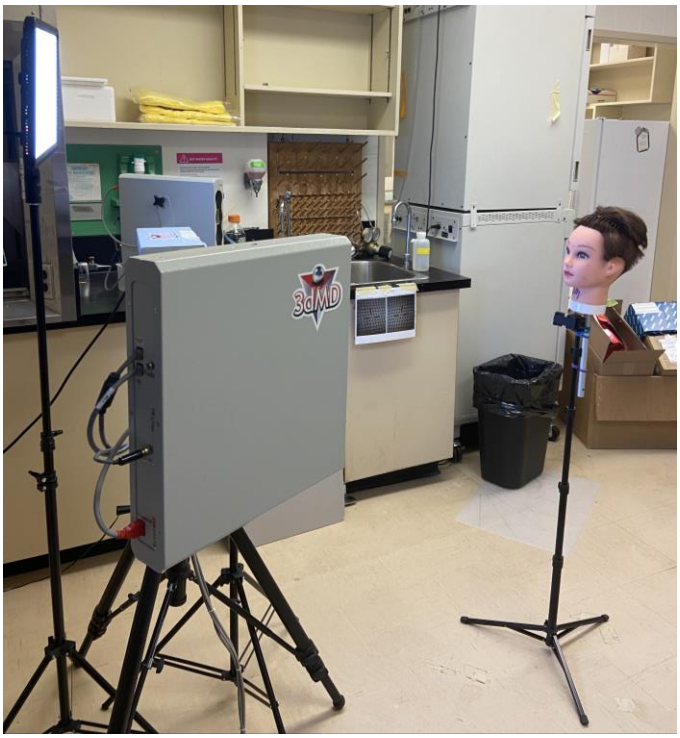

Figure 2.3: Bellus Arc7 Camera Set-up

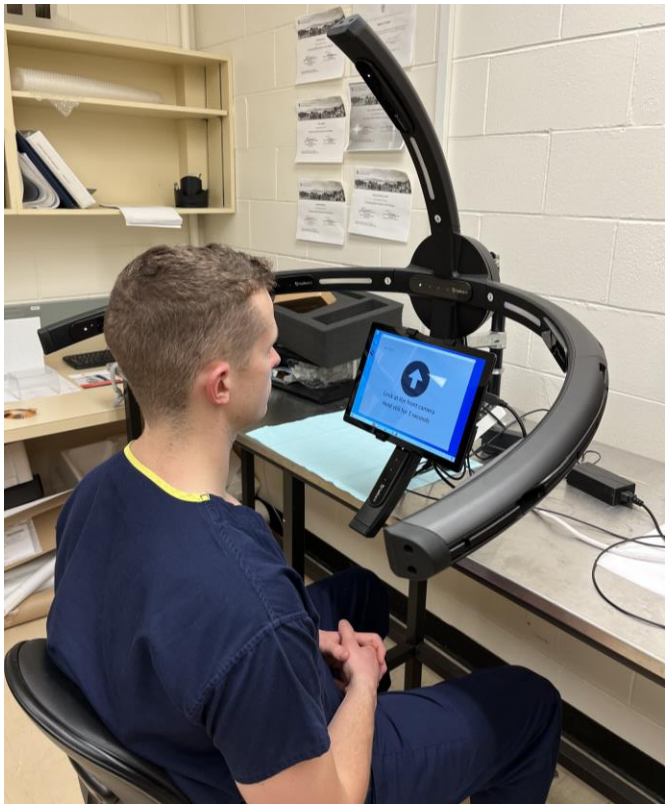

2.2.2 Part II

For each of the 14 subjects, five images were captured on the same day within an hour. Prior to scanning five Suremark Fiducial markers (VF-20 DentalMark 2.0mm) were applied to the patient's face (Figure 2.4). These markers were used to improve the capture of the forehead and nose region during extraoral scanning with the Trios intraoral scanner (3Shape, Copenhagen, Denmark). The five images were as follows:

1. Intraoral scan of the maxillary dentition including the palate with Trios (Figure 2.10C);
2. Extra-oral or perioral region including the labial surface of the upper front teeth, nose and the forehead with Trios (Figure 2.10B);
3. Facial scan in repose with Bellus Arc7 (Figure 2.10A);
4. Facial scan in repose with Artec Space Spider (Figure 2.10D);
5. Facial scan in maximum intercuspation retracted with Artec Space Spider (Figure 2.10E).

Each subject was given strict instructions prior to the image capturing to maintain the same standard throughout. All subjects were asked to lightly close their eyes during the capture of each of the five images for consistency as closed eyes were preferred during imaging with the Artec Space Spider scanner due to the strobe light.

As in Part I, both 3D facial scanner systems were assembled in the Digital Imaging Lab at the University of British Colombia's Dental Faculty. For each subject, the three facial images were captured in the same room, with the same lighting conditions within 10 minutes of each other. As for the two Trios intraoral scans these were captured in a dental chair in the Graduate Orthodontic Clinic within 30 minutes of the 3D facial scans.

Imaging for the Bellus Arc7 scanner was captured and processed the same as described in part I (see above).

The Artec Space Spider is an industrial portal handheld scanner. The scanner was preheated and calibrated according to the manufacturer's instructions. Each time the camera was moved to a new location the camera was recalibrated, which entails setting up the calibration kit and placing the scanner on top of the clear plastic stand (Figure 2.5). In Artec Studio software navigate to file and then run diagnostics tool. A new window opens and at the top of the toolbar select Start Calibration. When the computer prompts you add the calibration-board serial number. After the camera warms up, the calibration begins as the screen guides you through all the positions that appear on the calibration pattern. Be sure not to bump or move the scanner during the calibration process as you move the pattern from one position to the next or you will need to start the process from the beginning. The process is complete after the fifteen and final position has been scanned, and then you click apply calibration. The craniofacial region of each subject was captured during one scan.

Before starting each scan, the settings were confirmed, and the sensitivity was increased to three-quarters of the maximum value as this allowed capture of the dentition. Turning on the scanner starts with the preview mode, this allows the researcher to verify that the area of interest is within the field of view (FOV) and the scanner is the ideal distance away from the subject for accurate image capture. The Artec studio software indicates when most surfaces in the FOV are within the center of the range meter by colouring them in green, while red means the surfaces are too close to the scanner, blue means the surfaces are too far from the scanner and no colour means the surface is not being recorded. Once the subject's area of interest is in the FOV and at the ideal distance the investigator presses the same button on the scanner again to start capture. Artec Space

Spider scanner captures objects at a rate of 7.5 frames per second to ensure that adjacent frames areas overlap as you gradually move the scanner around the subject.

To ensure standardization, each subject was captured in the same manner by the same investigator, first by capturing the right ear then the right cheek, then moving up to the forehead, down the face capturing the buccal surfaces of maxillary anterior dentition and then down the chin and finally to the left cheek and finishing off at the left ear. Once the scan was captured the image could be moved, rotated, or scaled in the Artec Studio software to ensure complete capture of the desired regions/landmarks. Each subject had two scans taken: one repose scan and one retracted scan. Once both scans were captured, each was processed with the same three steps in the tools panel of the software before saving. The first step involved applying Global registration; this algorithm converts all one-frame surfaces to a single coordinate system using the information on the mutual position of each surface pair. Step two applied Outlier removal; this step eliminates outliers, which are small surfaces unconnected to the main surfaces. This process is based on an algorithm that calculates for every surface point the mean distance and standard deviation between that point and several neighbouring points. Step three is Sharp fusion. Fusion is the process that creates a polygonal 3D model, specifically sharp fusion algorithm perfectly reconstructs fine features. The final step is to save each of the individual sharp fusion scans as a mesh in the OBJ file format.

The maxillary dentition of each subject was captured with the Trios intraoral scanner. The scanner was calibrated as per manufacturer's instructions prior to scanning each subject. To calibrate the Trios intraoral scanner, one needs to remove the scanner tip and apply the calibration tip. On the Trios system go to the configure tab, select scan and then calibrate scanner and follow the on-screen instructions. Wait for the system to tell you the calibration process is complete,

which takes about 30 seconds, before removing the calibration tip and replacing it with the scanner tip.

Each participant was given clear instructions by the same investigator prior to scanning and the subject's teeth were dried with gauze. The first scan, which captured the maxillary dentition and palate alone, required the subject to remain still and keep his/her mouth open.
The second scan was captured with the patients' lips and cheeks retracted with teeth in maximum intercuspation and eyes gently closed. This scan captured the buccal surfaces of the maxillary dentition from canine to canine, the upper lip, philtrum, nose, and forehead. The fiducial markers helped improve the scan capture of poorly differentiated landmarks such as the forehead [23].
Prior to exporting the images as STL files, the scans were checked for any missing data in the regions of interest and re-scanning was performed if there were any significant gaps.
All recorded data sets were stored securely on a UBC dentistry hard drive. Each participant's data were analyzed separately.

Five subjects had the same five images repeated one week after their initial scans by the same researcher to assess the intra-operator reliability.

Geomagic Control X was used to analyze the images from part I and II of the study.

Figure 2.4: Placement of the Five Suremark Fiducial Markers

Figure 2.5: Artec Space Spider Calibration Set-up

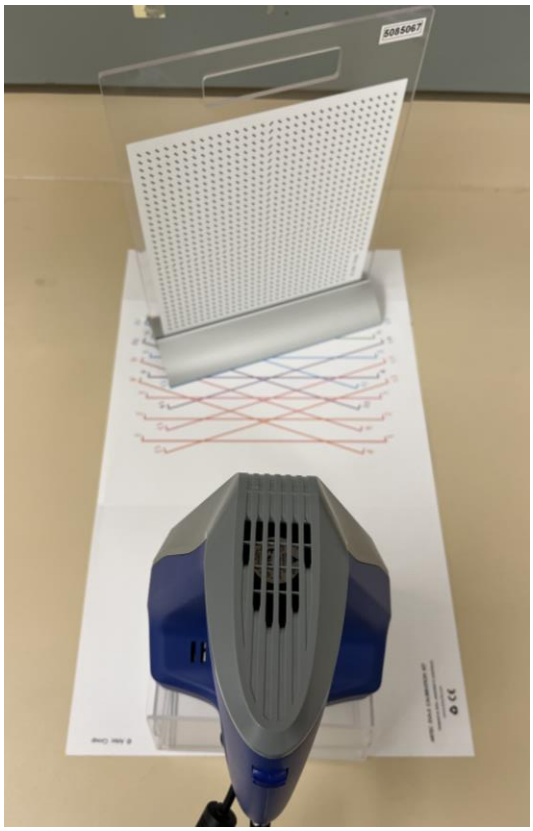

Figure 2.6: Artec Space Spider Camera Set-up

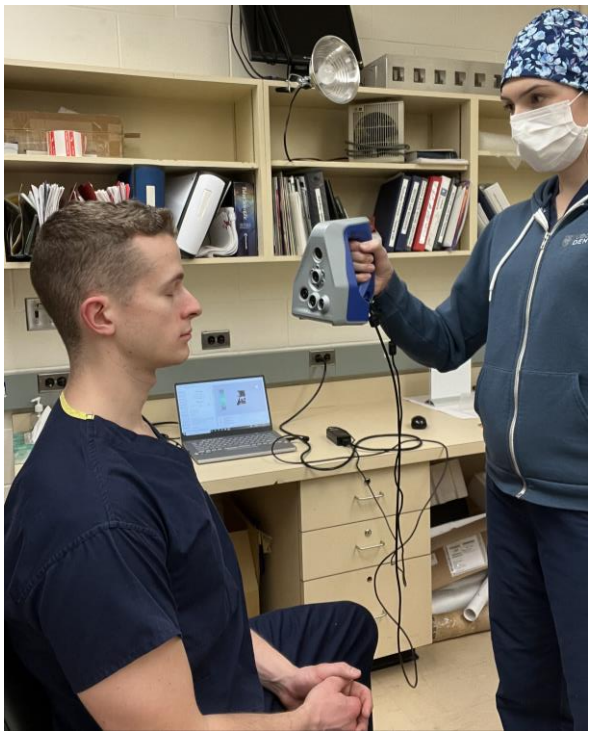

Figure 2.7: Trios Intraoral Scanner Set-up

2.3 Data Processing

2.3.1 Part I

The workflow for analyzing the facial scans is depicted in Figure 2.8. The 3dMDface system scan was imported into the software and designated as the reference scan data. The Bellus Arc7 face scan was imported into the software and designated as the measured scan data.

The reference scan was divided into three regions, as seen in Figure 2.9. The pink- and purple-coloured regions are the areas of interest. The orange-coloured region, which includes the neck, submental tissue and areas passed the hairline were not included due to a lack of complete capture and distortions. For a close approximation of the two facial scans, we used the software's iterative closest point algorithm. Then, we used the best-fit algorithm selecting the forehead and bridge of the nose region (purple-coloured section) as our surface area of registration (Figure 2.9).

Once the scans were aligned using the best-fit method, we performed the 3D comparison using the 3D compare statistics control X function to compare the mean deviation between the reference data and the measured data. This generated a 3D heat map for comparison. The overall deviations, indicated as the root mean square (RMS), were calculated and recorded utilizing the Geomagic Control X software report generator function. RMS was used as the measure of deviance versus using the mean as it provided a measure of absolute deviation between the two scans.

RMS: The Root Mean Square, which is a measure of the magnitude of all deviation values.

$$RMS = \sqrt{\frac{1}{n}\sum_{i=1}^{n} {D_i}^2}$$

Figure 2.8: Workflow - Part I

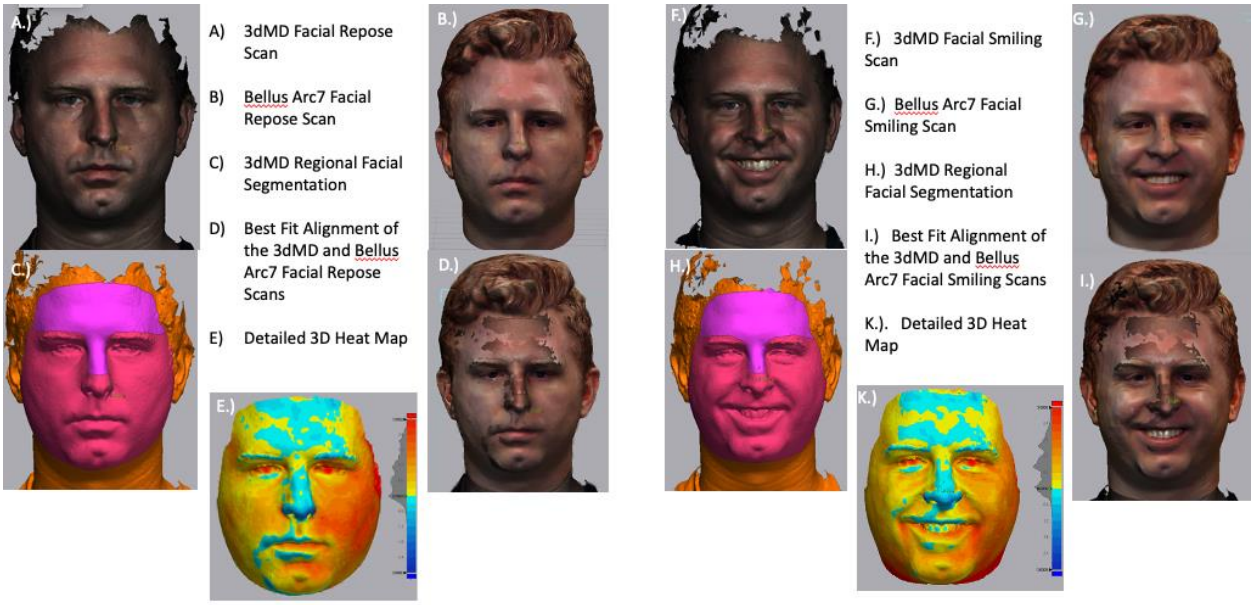

Figure 2.9: Reference Scan (3dMD) Depicting Regions for Superimposition and Analysis

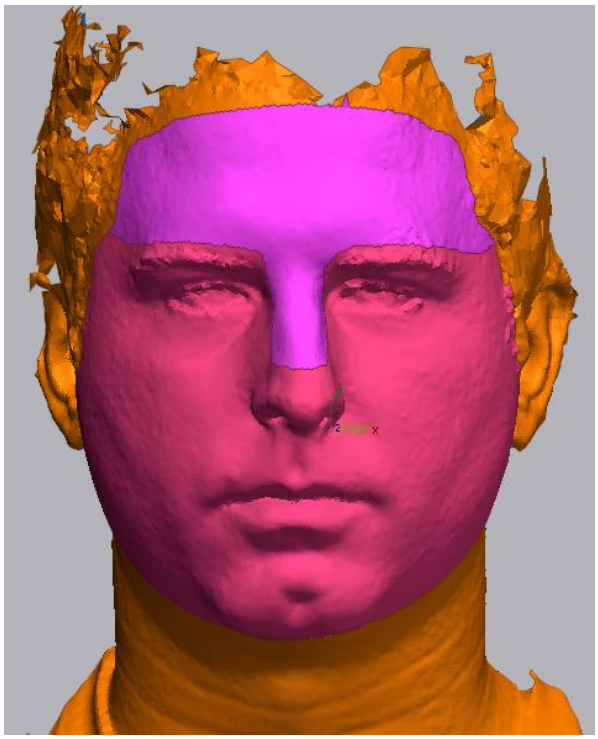

2.3.2 Part II

The workflow for analyzing the facial scans is depicted in Figures 2.10. For each subject, the three facial scans, one forehead/nose scan and two copies of the maxillary intraoral scan (designated as Upperteeth1 and Upperteeth2) were imported into the Geomagic Control X software.

For the experimental dataset, the Arc7 facial scan was superimposed to the Trios forehead/nose scan first using three landmark points on the forehead/bridge of the nose as depicted in Figure 2.11. This roughly aligns the two scans. After the initial alignment, the same two scans were aligned further using the Global and Fine registration function using a specific area on the forehead and bridge of the nose (Figure 2.12), this function leads to improved alignment of the two scans.

Next, the forehead/nose scan was aligned with the first copy of the intraoral scan, first using three landmark points as depicted in Figure 2.13, then again the same two scans were aligned using the Global and Fine registration function using the maxillary anterior teeth (canine to canine) as shown in Figure 2.14. After each superimposition, Geomagic Control X software provides a mean deviation between the two scans, which was checked by the investigator for any major inconsistencies.

Finally, the Arc7 facial scan and first copy of the upper teeth scan were combined into a single superimposed image (Figure 2.15).

The same steps were followed for the reference dataset. The Artec Space Spider facial scan repose was initially aligned using three landmarks on the forehead/bridge of nose to the Artec Space Spider facial scan retracted (Figure 2.16). These scans were realigned using the Global and Fine registration function using a specific area on the forehead and bridge of nose (Figure 2.17).

Next the Artec Space Spider facial scan retracted was aligned to the second copy of the maxillary intraoral scan first using three landmarks on the upper teeth (Figure 2.18) and then again using Global and Fine registration function using the maxillary anterior teeth (canine to canine) as shown in Figure 2.19. Finally, the Artec Space Spider facial scan repose and second copy of the upper teeth scan were combined into a single superimposed image (Figure 2.21).

Next the superimposed reference data was sectioned into compartments highlighted in Figure 2.22.

The silver- and olive-coloured regions are the areas of interest, including the maxillary teeth. The dark green coloured region, which includes the neck, submental tissue and areas passed the hairline was not included due to a lack of complete capture and distortion in the facial scans. The combined Artec Space Spider image was designated as the reference data and the combined Arc7 image was designated as the measured data. For a close approximation of the two facial scans, we used the software's iterative closest point algorithm. Then, we used the best-fit algorithm selecting the forehead and bridge of the nose region as our surface area of registration (Figure 2.23).

As in part I dataset, once the scans were aligned using the best-fit method, we performed the 3D comparison using the 3D compare statistics control X function to compare the deviation between the reference data and the measured data, this generated a 3D heat map for comparison (Figure 2.24). Next, five points were selected in the maxillary arch to look at the specific point-to-point comparisons. For each individual's 3D heat map the mesial buccal cusp of the right and left first molar, the incisal tip of the right and left canines and the incisal/palatal surface between the central incisors were selected. The overall deviations (RMS) were calculated and recorded utilizing the Geomagic Control X software report generator function.

Figure 2.10: Workflow - Part II

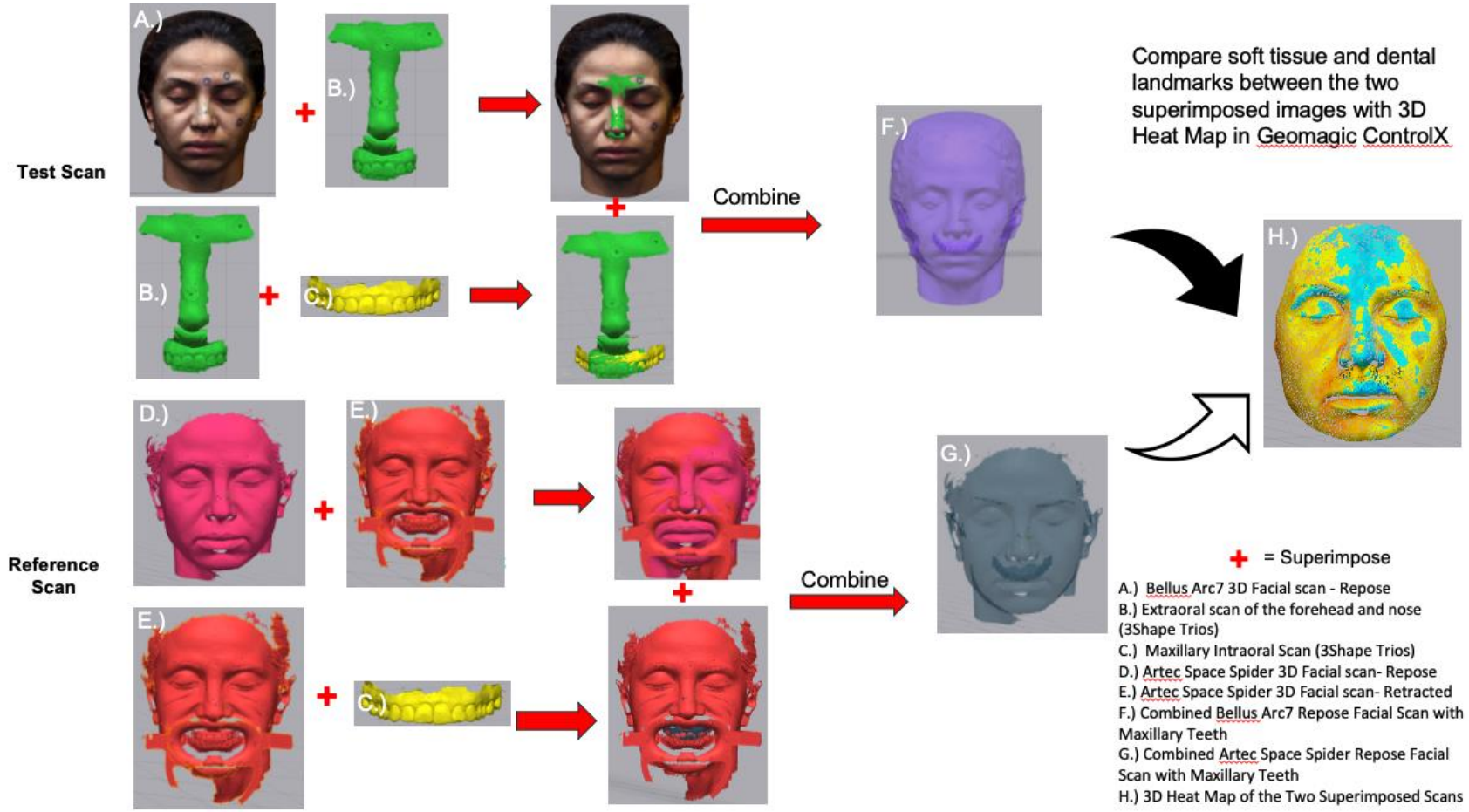

Figure 2.11: Landmark-based Registration between Arc7 Facial Scan and Trios Extraoral Scan

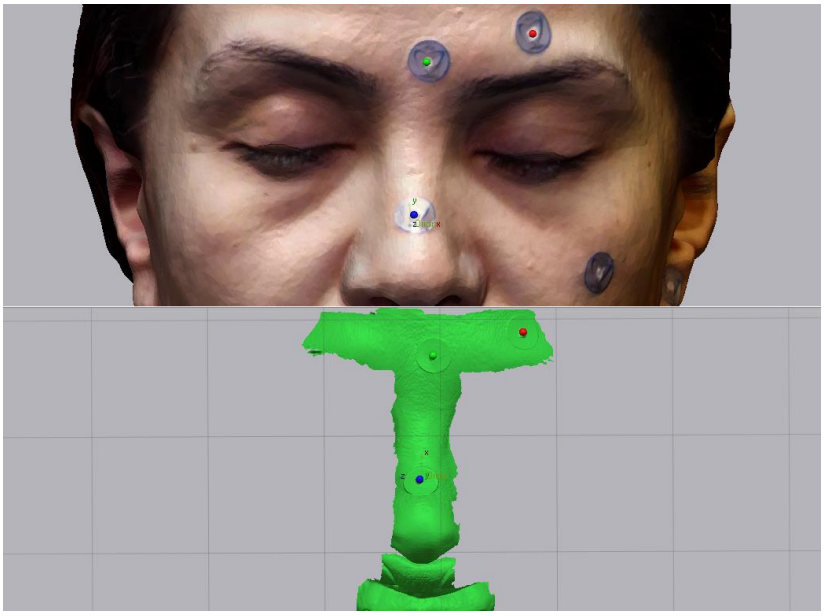

Figure 2.12: Surface-based Registration between Arc7 Facial Scan and Trios Extraoral Scan

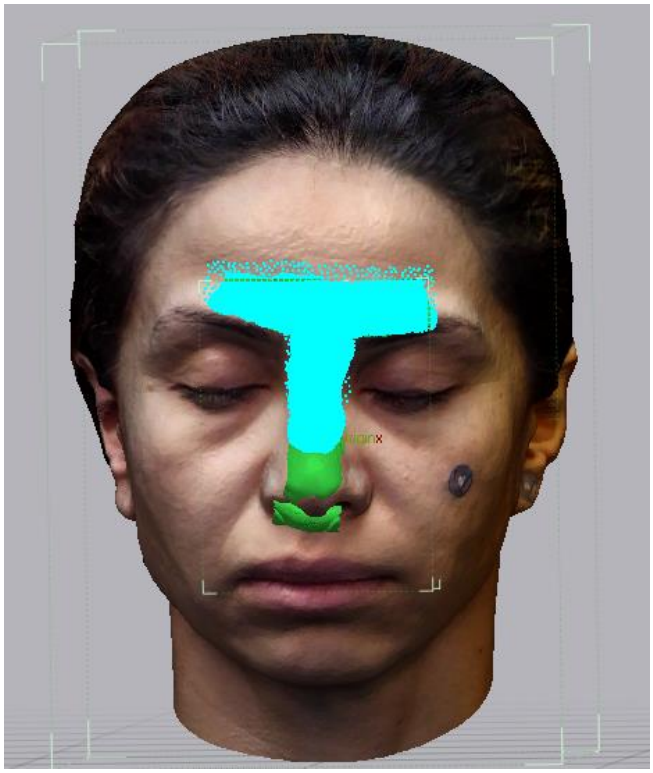

Figure 2.13: Landmark-based Registration between Trios Extraoral Scan and Trios Intraoral Scan

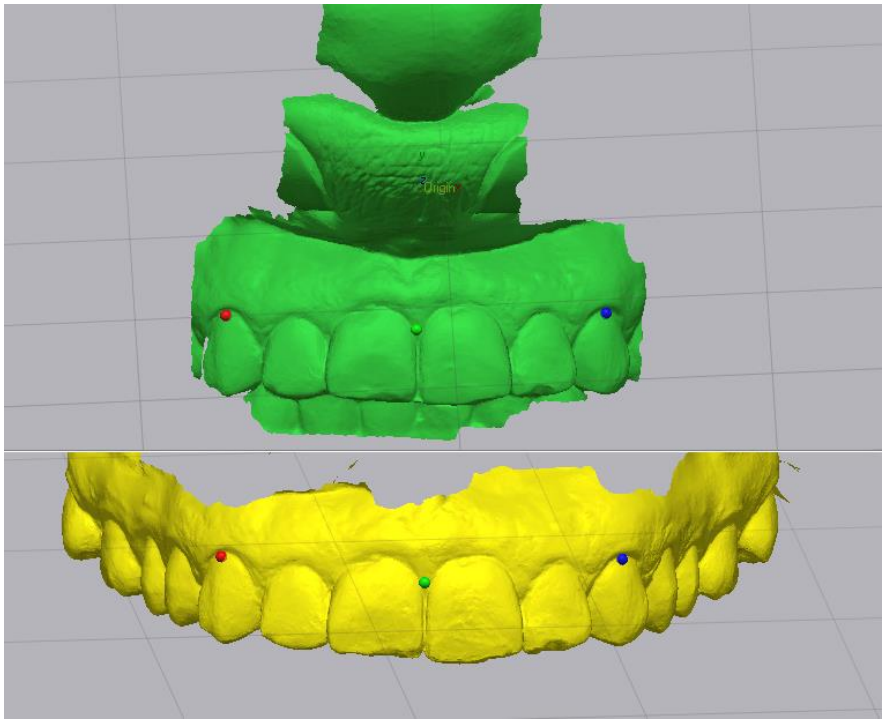

Figure 2.14: Surface-based Registration between Trios Extraoral Scan and Trios Intraoral Scan

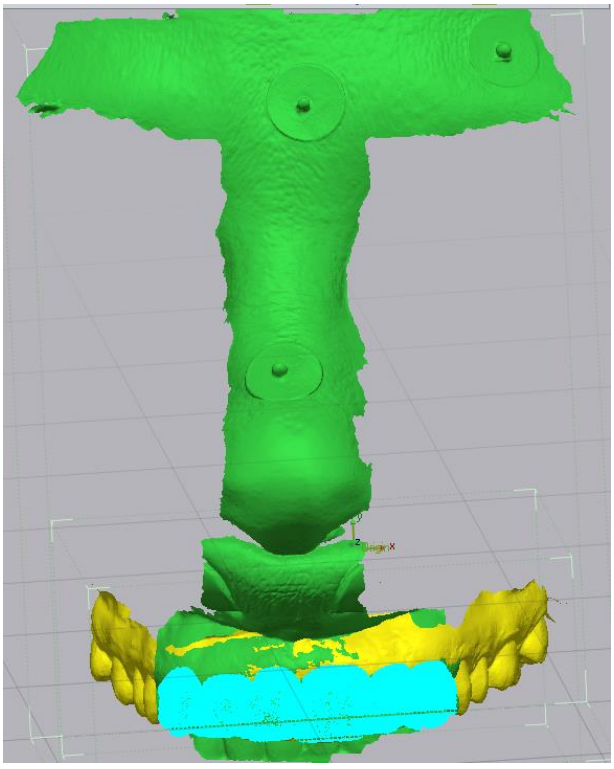

Figure 2.15: Superimposed Arc7 Repose and Trios Scans Without and With Transparency

Figure 2.16: Landmark-based Registration between Artec Space Spider Repose and Retracted Scans

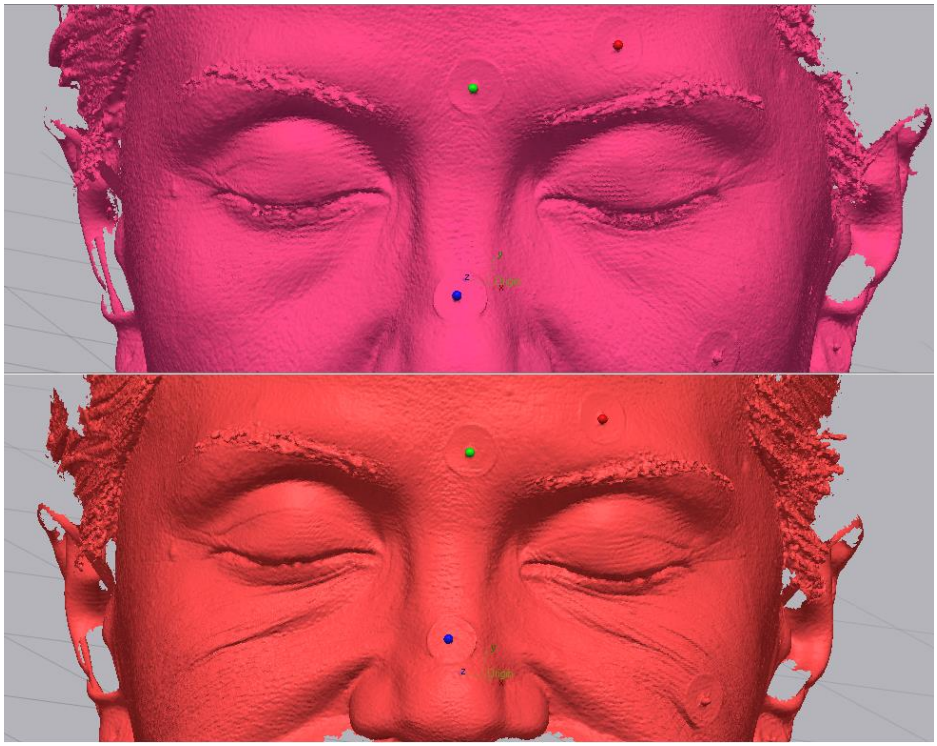

Figure 2.17: Surface-based Registration between Artec Space Spider Repose and Retracted Scans

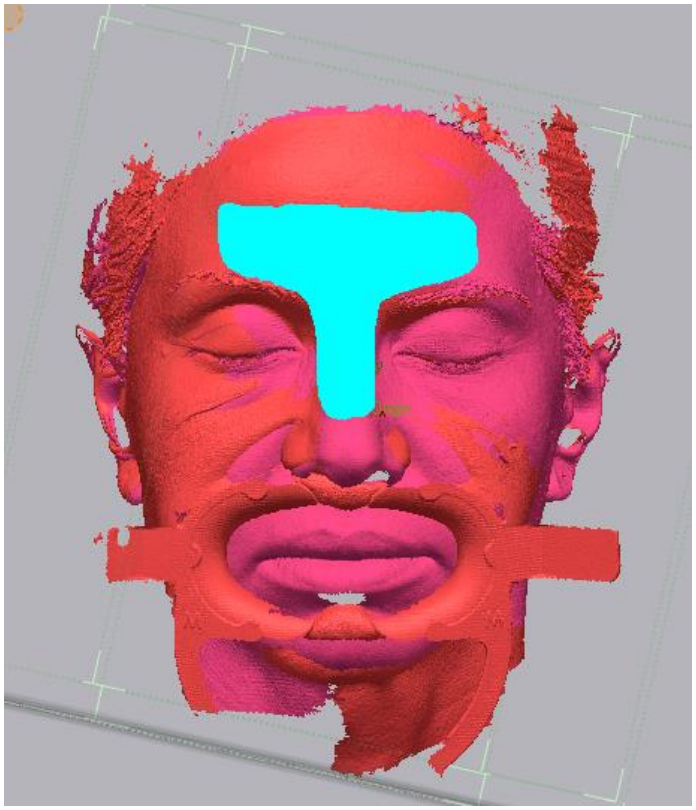

Figure 2.18: Landmark-based Registration between Artec Space Spider Retracted and Trios Intraoral Scan

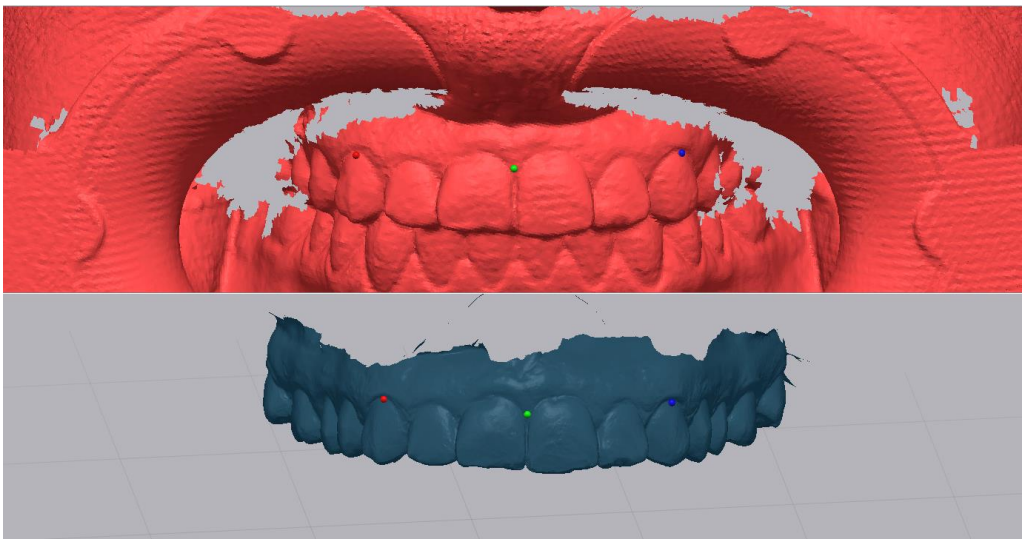

Figure 2.19: Surface-based Registration between Artec Space Spider Retracted and Trios Intraoral Scan

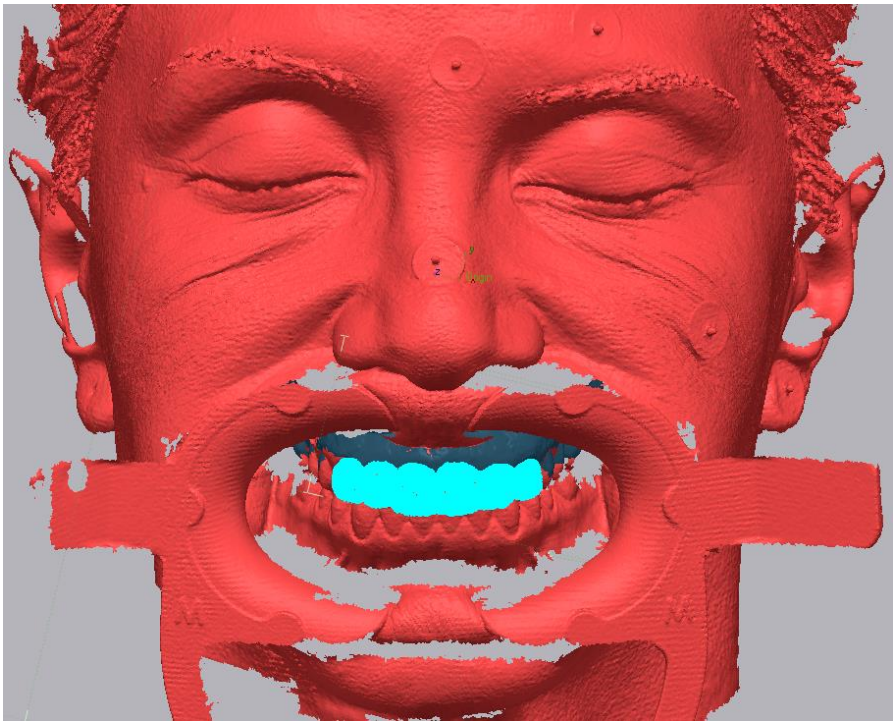

Figure 2.20: Superimposed Artec Space Spider Retracted and Trios Intraoral Scan

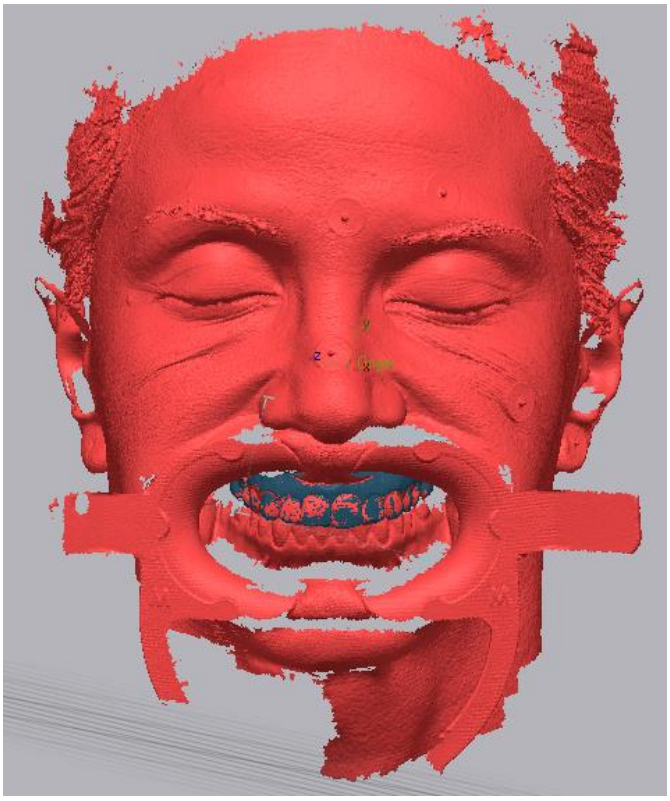

Figure 2.21: Combined Artec Space Spider Repose and Trios Intraoral Scans (With Transparency)

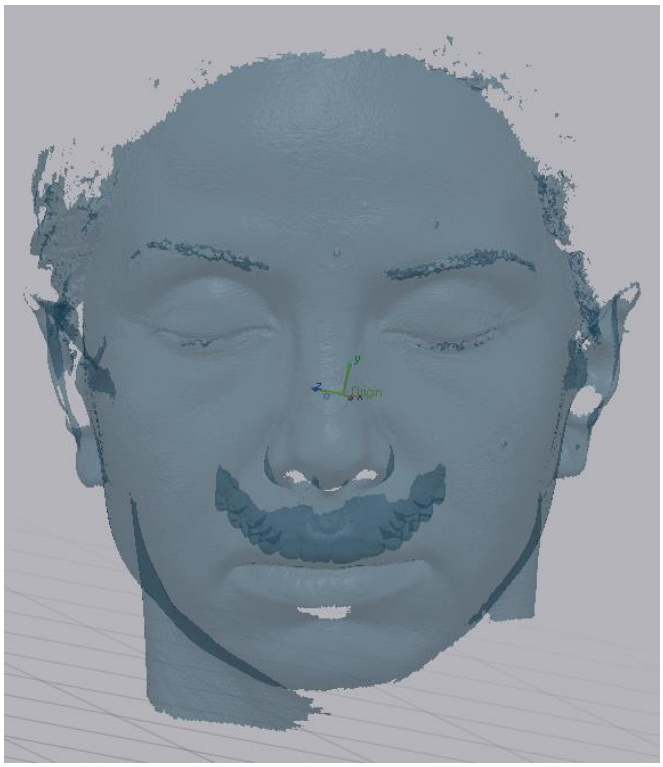

Figure 2.22: Reference Scan (Artec Space Spider) Depicting Regions for Superimposition and Analysis (Without and With Transparency)

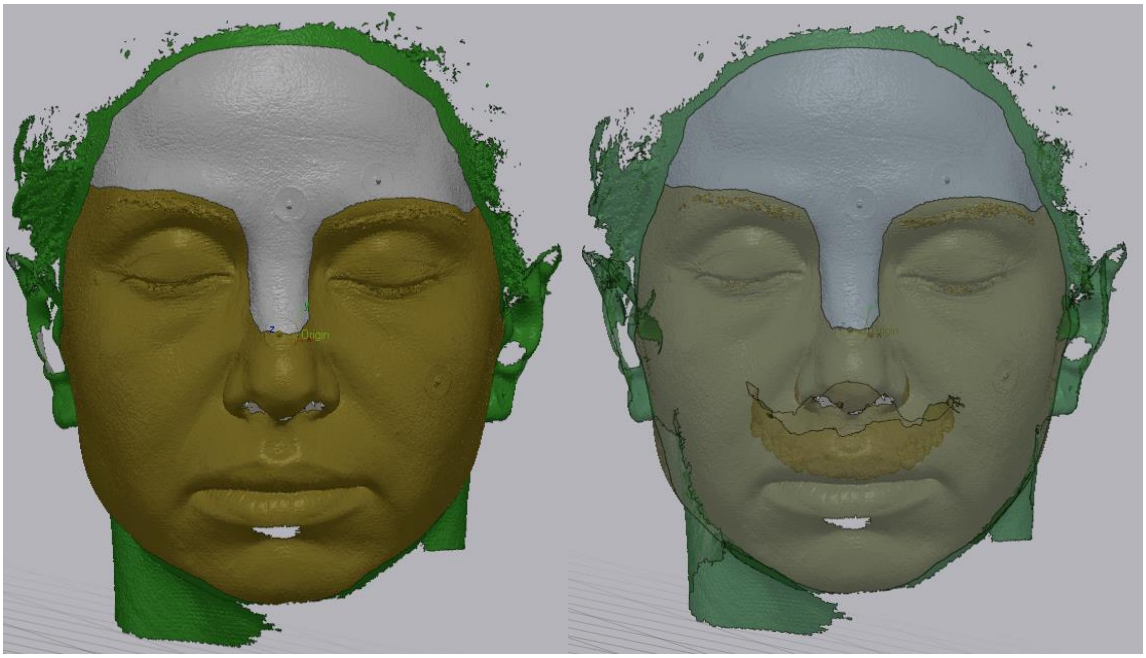

Figure 2.23: Superimposed Facial Scans Using the Best Fit Algorithm

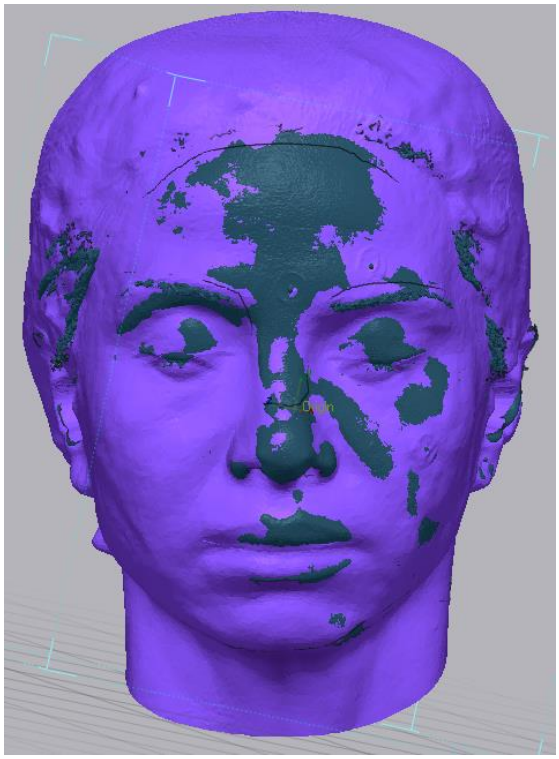

Figure 2.24: Detailed 3D Heat Map

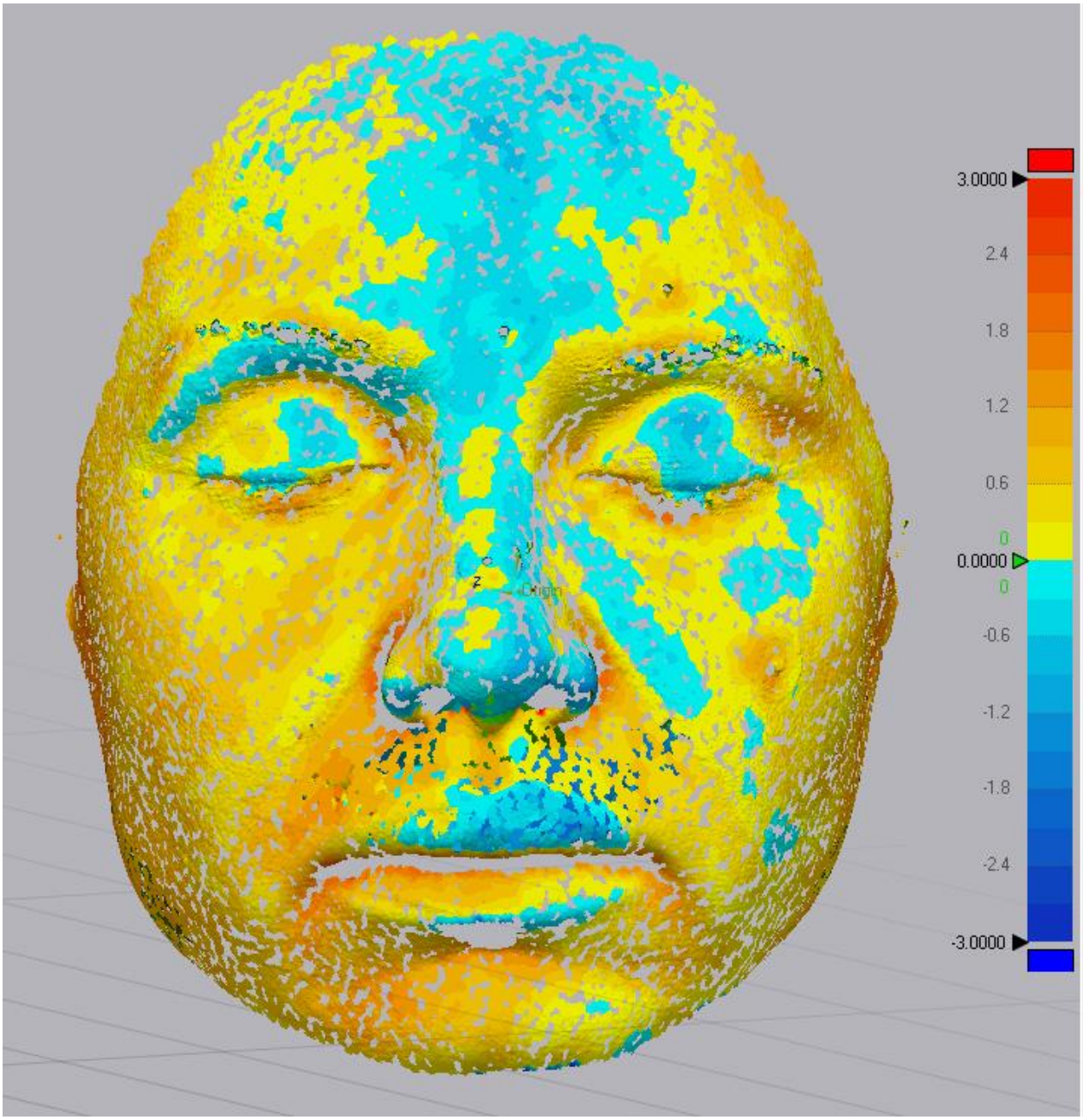

Figure 2.25: Analysis of Superimposition. Frontal and Left and Right Lateral Views. Note: Green areas signify error < 2mm.

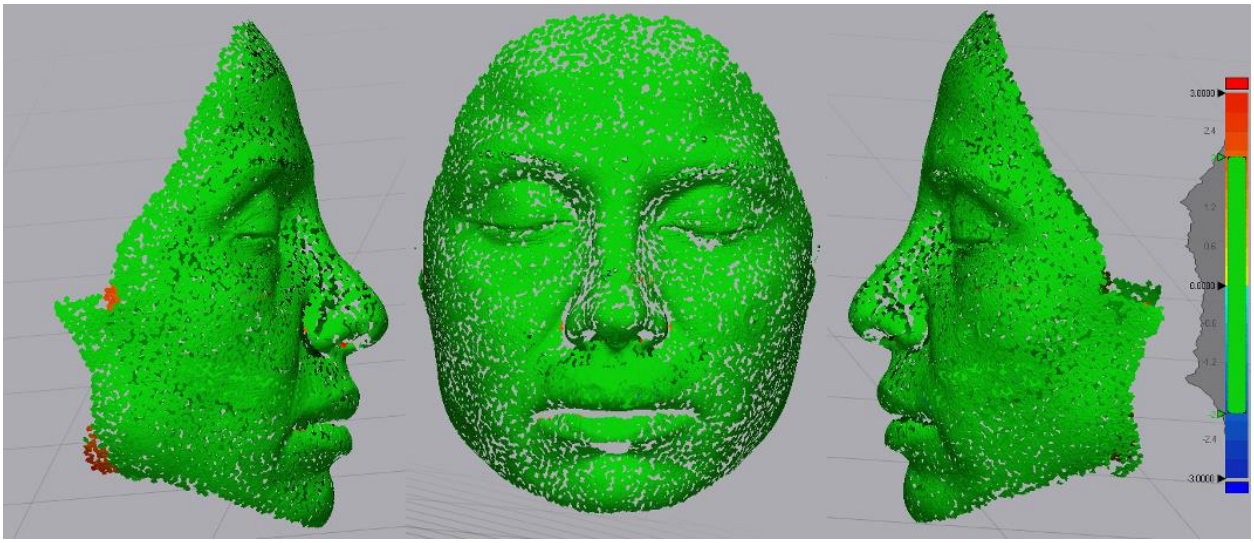

Figure 2.26: Analysis of Superimposition. Inferior View. Green areas signify error < 0.5 mm.

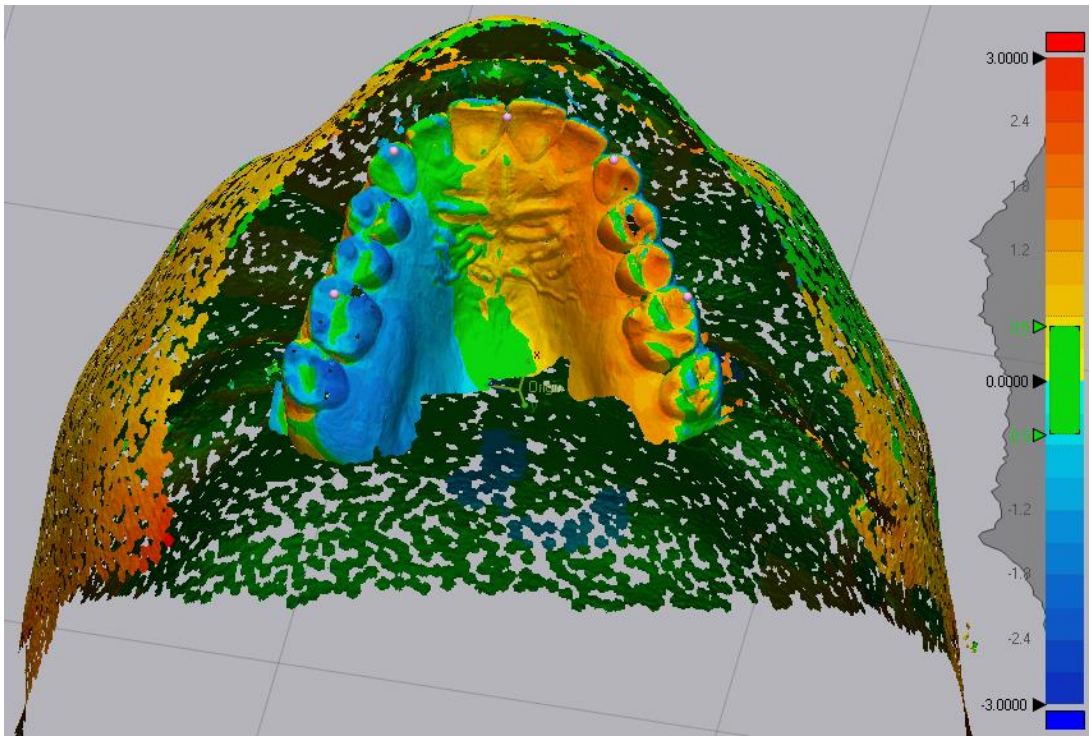

2.4 Quantitative Analysis

In our study, level of accuracy describes the amount a specific measurement deviates from its actual or "true" value. Therefore, in part I of the study, accuracy was analyzed by comparing the measurement acquired from 3D facial images of three subjects constructed from the Bellus Arc7 system to the "true" value measurements obtained from our reference camera, the 3dMD system. To show and analyze the discrepancies present we used the overall mean RMS distance.

For part II of our study, accuracy was analyzed by comparing the overall mean surface-to-surface root mean square distance for facial and the mean point-to-point distance for dental measurements acquired from superimposed 3D facial images of 14 subjects constructed from the Bellus Arc7 system to the "true" value measurements obtained from our reference camera, the Artec Space Spider system. Precision or reliability describes the difference in measurements of images taken repetitively of one participant. Therefore, in part I of the study, precision was evaluated by comparing the repeat measurements of the same three subjects 1 week later. For part II of the study, precision was represented by comparing repeat measurements of five subjects 1 week later.

2.5 Statistical Methods

Statistical data analysis was performed using the statistical software program (IBM SPSS Statistics, Version 29.0; IBM Corp).

2.5.1 Part I

For part I, a descriptive analysis was applied to the measure of deviance calculated as the surface-to-surface RMS distance between the measured data, Bellus Arc7 camera and the reference data, the 3dMDface system.

The intraclass correlation coefficient (ICC) is a measure of reliability, which reflects the degree of correlation and agreement between two repeated measurements. ICC values for reliability range from 0-1, where values closer to 1 represent stronger reliability [24]. Intra-rater reliability was measured using the intra-rater reliability coefficient and graphically depicted using the Bland-Altman plot [25]. ICC values were interpreted according to Koo and Li's [24] recommendations which state that values less than 0.5 represent poor reliability, between 0.5-0.75 represent moderate reliability, between 0.75 to 0.90 represent good reliability and above 0.90 represent excellent reliability.

2.5.2 Part II

For part II, a descriptive analysis was performed with the measure of deviance calculated as the surface-to-surface RMS distance between the measured data for the superimposed Bellus Arc7 camera and the superimposed reference data, Artec Space Spider. We also reported point-to-point measurements of deviation from five specific points in the dentition (mesial buccal cusp of right and left first molar, cusp tip of right and left canine, and incisal-palatal point between the two maxillary centrals). The same investigator repeated the same five scans in five subjects to examine the intra-rater reliability. Intra-rater reliability was measured using the ICC and graphically depicted using the Bland-Altman plot.

Chapter 3: Results

3.1 Part I

Table 3.1 outlines the RMS distance and standard deviation for all the participants and was calculated to quantify the overall accuracy of the Bellus Arc7 scanner. The overall root mean square deviance for Arc7 as compared to the reference 3dMD was 1.16 mm ± 0.41 mm. The RMS was below 2 mm for all three subjects, which is clinically acceptable for soft tissue measurements.

Repeat measurements for each of the three subjects 1 week later revealed the mean deviance was -0.24 mm ± 0.26 mm.

The intraclass correlation coefficient (a measurement of reliability within a single observer) [25] was 0.87, which is classified as good. (Table 3.2) A Bland-Altman plot graphically depicts the intraclass correlation coefficient (Figure 3.1).

Table 3.1: Part I – Overall Surface-to-Surface Deviation per Participant

Participant ID	Root mean square (mm)	Standard Deviation	95% Confidence Interval (Upper limit)	95% Confidence Interval (Lower limit)
1	0.46	0.45	1.34	-0.42
2R	1.49	0.99	3.43	-0.45
2S	1.36	0.86	3.05	-0.33
3R	1.31	0.88	3.03	-0.41
3S	1.18	0.98	3.10	-0.74
Overall	**1.16**	**0.41**		

Table 3.2: Part I – Intraobserver Reliability

Participant ID	RMS Timepoint 1	RMS Timepoint 2	Difference	Mean
1	0.46	0.53	-0.08	0.5
2R	1.49	1.44	0.05	1.47
3R	1.31	1.93	-0.62	1.62
2S	0.86	1.31	-0.21	1.46
3S	0.98	1.28	-0.36	1.36
Overall				**-0.24**

Figure 3.1: Bland-Altman Plot Comparing the Repeated Timepoints Part I

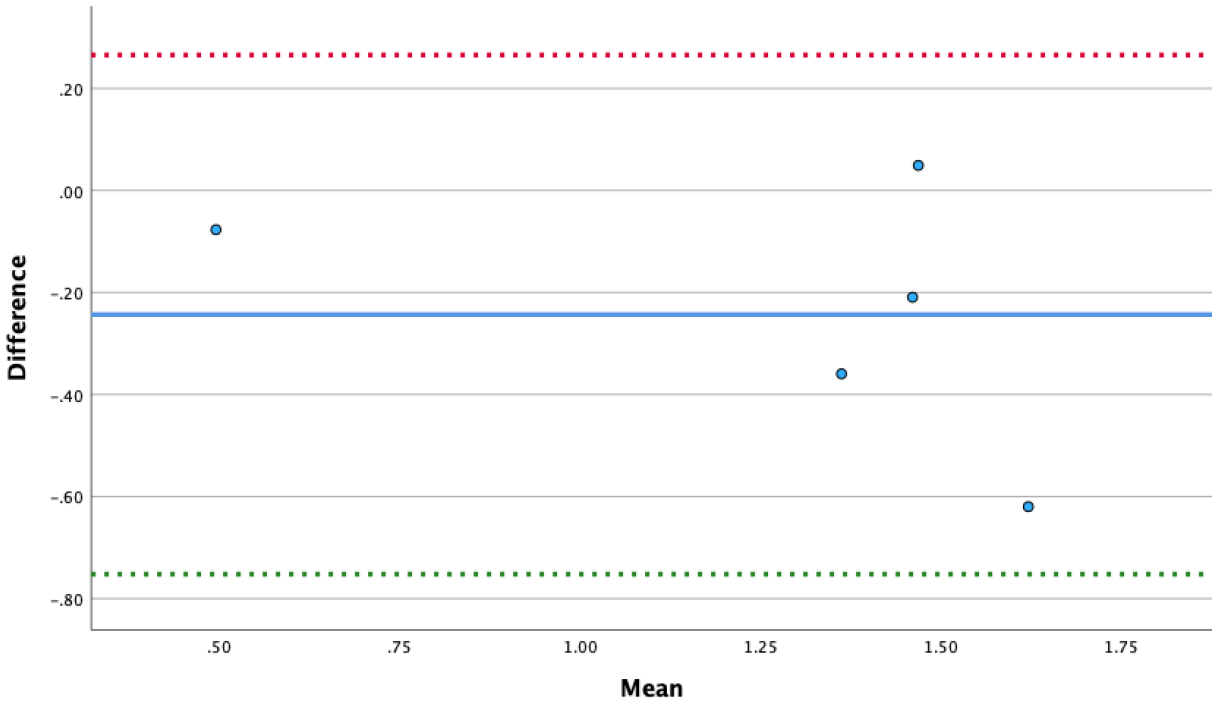

3.2 Part II

Table 3.3 outlines the RMS distance and the standard deviation for all the participants and was calculated to quantify the overall accuracy of the superimposition method using the Bellus Arc7 scanner and the novel method of merging scans from an extra-oral scan of the forehead, nose and maxillary teeth using the Trios scanner. The overall RMS was 1.52 mm ± 0.54 mm.

Table 3.4 shows the total deviance by specific tooth landmarks. The mean deviance for molar left was 0.09 mm ± 1.98 mm. The mean deviance for molar right was -0.76 mm ± 1.97 mm. The mean deviance for canine left was 0.18 mm ± 1.50 mm. The mean deviance for canine right was -0.48 mm ± 1.30 mm. The largest deviance was seen for the palatal-incisal landmark between the two central incisors, which had a mean of 1.03 mm ± 1.38 mm.

Figure 3.2 shows a sample of six subjects with detailed 3D heat maps of the soft tissue generated after best-fit alignment. Figure 3.3 shows a sample of six subjects with detailed 3D heat maps of the dentition generated after best-fit alignment.

Table 3.5 shows the root mean square distances for timepoint 1 and timepoint 2 for the five subjects that had repeat scans 1 week apart. The ICC was 0.55, which is classified as moderate. A Bland-Altman plot graphically depicts the intraclass correlation coefficient (Figure 3.3).

Part II showed that integrating intraoral scans with 3D facial images to create a 3D patient was possible using this novel merging method, albeit very technique sensitive.

Table 3.3: Part II - Overall Surface-to-Surface Deviation per Participant

Patient ID	Root mean square error (mm)	Standard Deviation	95% Confidence interval (Upper limit)	95% Confidence interval (Lower limit)
1	1.31	1.31	3.87	-1.26
2	1.21	1.17	3.49	-1.08
3	0.80	0.61	2.00	-0.40
4	1.74	1.64	4.95	-1.48
5	1.51	1.51	4.46	-1.45
6	1.15	0.96	3.03	-0.74
7	1.12	1.12	3.32	-1.07
8	1.93	1.93	5.71	-1.85
9	2.45	1.91	6.20	-1.30
10	1.07	0.89	2.82	-0.67
11	2.37	1.98	6.24	-1.51
12	1.79	1.45	4.62	-1.05
13	1.10	0.99	3.05	-0.84
14	0.95	0.87	2.66	-0.75
Overall	**1.52**	**0.54**		

Table 3.4: Part II - Dentition Point-to-Point Deviation

Dental Point	Mean (mm)	Standard Deviation	95% Confidence interval (Upper limit)	95% Confidence interval (Lower limit)
Molar Left	0.09	1.98	1.24	-1.05
Canine Left	0.18	1.50	1.04	-0.69
Incisor	1.03	1.38	1.83	0.23
Canine Right	-0.48	1.30	0.27	-1.23
Molar Right	-0.76	1.97	0.38	-1.90

Figure 3.2: Sample of Six Subjects Soft Tissue 3D Heatmap (Threshold deviation ± 3mm)

Figure 3.3: Sample of Six Subjects Dentition 3D Heatmap (Threshold deviation ± 2mm)

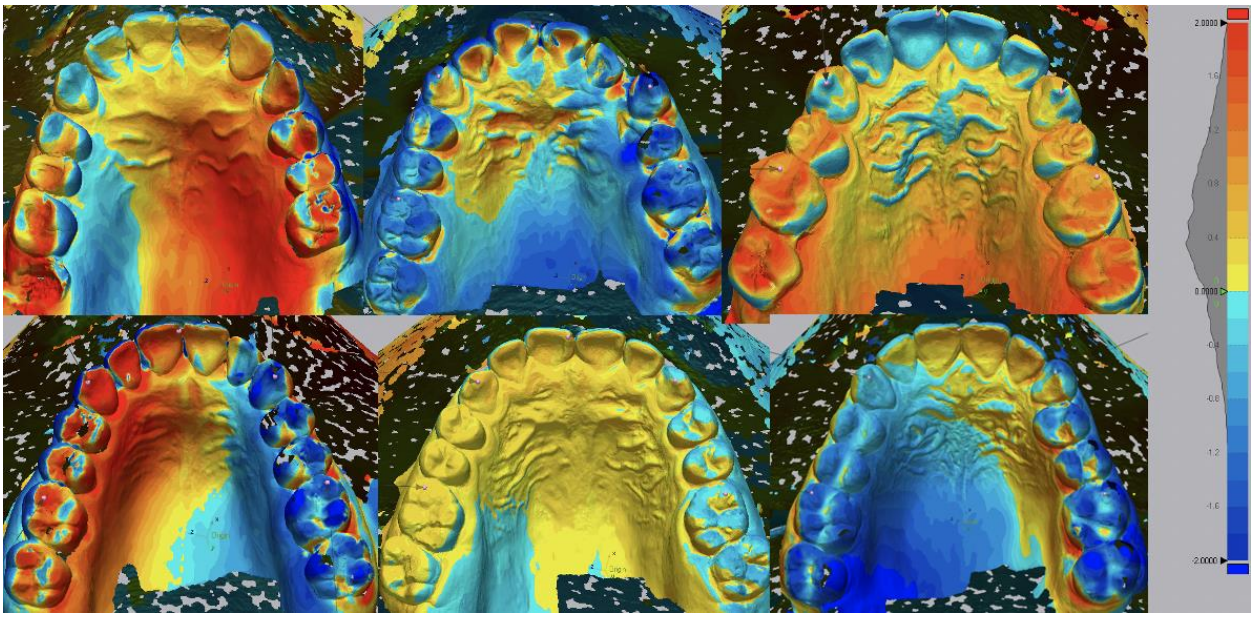

Table 3.5: Part II - Intraobserver Reliability

Patient ID	RMS Timepoint 1	RMS Timepoint 2	Difference	Mean
2	1.21	0.59	0.62	0.90
5	1.51	0.82	0.68	1.17
7	1.12	1.26	-0.14	1.19
8	1.93	1.11	0.82	1.52
13	1.10	1.57	-0.47	1.34

Figure 3.4: Bland-Altman Plot Comparing the Repeated Timepoints Part II

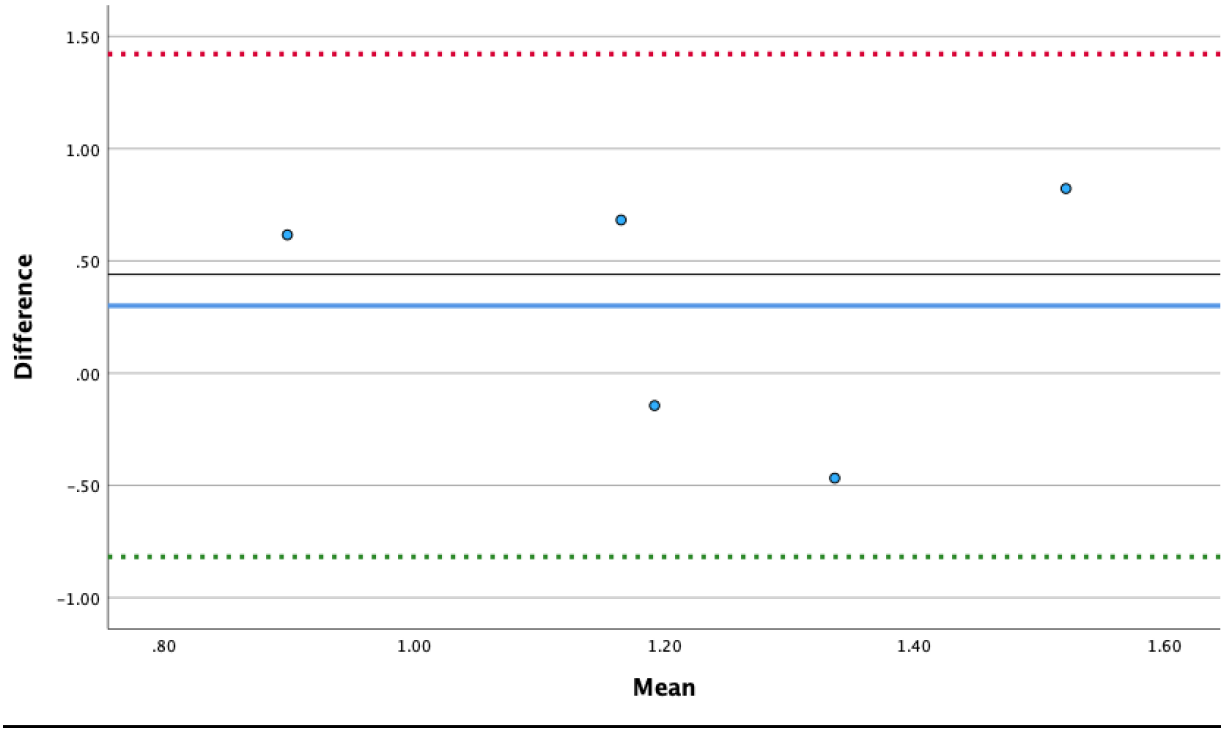

Chapter 4: Discussion

In orthodontics and craniomaxillofacial surgery, the assessment and analysis of the key tissue groups referred to as the triad (facial soft tissue, facial skeleton, and dentition) are essential for diagnosis and treatment planning [1], [15]. 3D data can greatly assist clinicians with their daily clinical practice regarding customized treatment planning, outcome simulation and patient education but currently, none of the 3D scanners on the market can accurately capture the complete triad. In addition, there is no gold standard method for merging 3D datasets [13]. Innovations in digital technology in the field of healthcare, including dentistry, have led to an influx of research on the creation of a 3D virtual patient [15], [26]. Marradi *et al.*, [15] 2020 systematic review selected 21 studies that created a virtual patient through superimposition of 3D data. Of these 21 studies, 90% were published in the last decade and 52% within the last five years. 3D facial scanning is advantages as it is a non-invasive method that requires minimal chair time, improves patient comfort, in addition to not requiring radiation [26]. The creation of a virtual patient is dependent on integration of two or more datasets, often different file types. Thus, it is important to have a reliable and accurate method for merging the datasets either by point-, surface- or voxel-based fusion methods [13].

For Part I of the study, the 3dMDface system was chosen as a reference standard against which the Bellus Arc7 scanner was compared, as previous studies have shown its accuracy to be within 1mm when compared with conventional anthropometric measurements [4], [9], [27]. RMS was computed as a measure of overall accuracy, relative to the 3dMD system. According to Aung *et al.*, 1995 [28] who compared the reliability of indirect facial measurements of the craniofacial complex to the gold standard of direct anthropometric measurements, reliability was

classified into four categories. Highly reliable when the deviation is less than 1.0mm, reliable when the deviation is less than 1.5 mm, moderately reliable when the deviation is between 1.5-2.0 mm and unreliable for anything beyond 2.0 mm [28], [29]. Our findings show the deviations from the reference standard were within the limits of clinical acceptability of 2mm for soft tissue measurements. While the Arc7 is less expensive, easier to use and calibrate than the 3dMD, and it also performed reasonably well, but it lacks the ability to capture complex structures and areas of high curvature.

For Part II of the study, we tested a novel merging method for integrating IOS with 3D facial scans without the use of dental scanning bodies. We chose the Artec Space Spider as our reference scanner as this handheld portal scanner has been repeatedly tested and it is precise and accurate in capturing the dentition [30]–[32]. Our study demonstrates that it is feasible to integrate IOS and 3D facial scans using the forehead and the bridge of nose as a reference, although such strategy is technique sensitive and has a steep learning curve. For our trained investigator the five images of each subject could all be captured within 30 minutes, while the superimposition of the images to create a 3D virtual model could be completed within 40 minutes.

The RMS for the overall surface-to-surface registered region was 1.52 mm ± 0.54 mm. However, the overall deviation for the dental landmarks showed a wide range. The mean deviance for molar left was 0.09 mm ± 1.98 mm while the mean deviance for molar right was -0.76 mm ± 1.97 mm. The mean deviance for canine left was 0.18 mm ± 1.50 mm while the mean deviance for canine right was -0.48 mm ± 1.30 mm. The largest deviance was seen for the palatal-incisal landmark between the two central incisors, which had a mean of 1.03 mm ± 1.38. Rangel *et al.,* [18] used the average distance between the matched surfaces of the maxillary

incisors to indicate the accuracy of integration, which was 0.35 ± 0.32mm. However, since this reference area is in the flat plane along the buccal surface this may only represent deviations in one dimension, and consequently may not detect errors in other dimensions. Xiao *et al*., [33] used a two-step method to integrate digital maxillary dental casts with 3D facial images, using CBCT scans as their reference and found that the mean absolute deviations for the full dentition were within 0.42 mm in all three dimensions. They concluded that the integration errors were larger in the molar region, z-orientation for translation and in the pitch orientation for rotation. One possible explanation for the wide range of deviations concerning the dental landmarks seen in our study could be patient movement. If during the extra-oral scan, the subject moves their upper lip then this can lead to an inaccurate position of the maxillary anterior teeth in relation to the forehead. For subjects whose 3D heat maps had the largest dental landmark deviations when we viewed the superimposed maxillary teeth as compared to the reference scan, we found that there was repeatedly a horizontal discrepancy and occasionally a cant in the occlusion. In addition, for some subjects we were unable to capture a continuous scan from the maxillary anterior teeth to the forehead at the region of upper lip when the lip was retracted due to their specific lip to nose morphology. In these specific cases, we could not use their records as the maxillary teeth were separated from the bridge of nose/forehead region upon exporting the STL file.

Another limitation of this novel merging technique is the multiple steps of image superimposition, which can introduce accumulated measurement errors. At each step we tried to control for this by ensuring the smallest overall deviation possible between the two superimposed scanned. Deviations ranged from as small as 0.02 mm, to as large as 0.37mm in our study. The largest deviations were seen when superimposing the perioral scan to the Bellus

Arc7 repose scan, minimal deviations were seen for the other superimpositions. Further advancements in scanning technology will reduce the need for multi-step superimpositions. An additional drawback of the tested merging method was due to the vertical limit of th*e Trios* scanner during perioral scanning. During our initial protocol testing phase, we quickly realized that there was a vertical and horizontal limit for the Trios scanner. We contacted 3Shape Company regarding this limitation, but they would not provide us with any information, stating that they do not recommend using the device for extra-oral scanning purposes. We decided to examine the vertical limit by repeat testing on a mannequin head and found the threshold to be roughly 13cm (Figure 4.1). Subjects with a relatively long-face and/or large nose had only a small portion of their forehead captured during the scan, while subjects with a relatively short-face and/or small nose had a much larger portion of their forehead captured. This inconsistency may have led to a difference in the accuracy of the merging technique between subjects. Another limitation is the operator's continued improvement with scanning and the integration protocol. Of importance, for every scanned subject the operator becomes faster with each scan. The reduced capture time can improve the accuracy and minimize the number of involuntary movements of the subject during the scan.

One of the disadvantages of the Artec Space Spider is the strobing structured light flashes that may make it difficult for the patient to fully relax their eyes during the scanning [31]. Especially in young subjects, it can be very difficult to hold the same position throughout the capture time. In Figure 3.2, which shows a random sample of six 3D heat maps, one can see larger deviations in the eyes and lip regions, most likely from subject's micro-movements. Some of the advantages of this 3D merging method include no radiation or risk to the patient, no requirement of additional dental scanning attachments and the scan can easily be completed in

any office that has access to an intraoral scanner and 3D facial scanner. While our study has proven that it is possible to use this novel method to create a virtual 3D patient, further studies and improvement in the protocol are required for this procedure to be valuable in an orthodontic clinical setting. As we have discussed above, not only is this protocol technique sensitive, but it is also not suitable for all patients. For example. young children who cannot hold still for the duration of the scan, orthognathic surgical cases where high accuracy and precision is required, patient with craniofacial anomalies and patients who do not want to remove their facial hair.

Although the sample size of previous studies investigating the creation of a 3D virtual patient through superimposition of 3D data has ranged from 1 to 30 subjects, a limitation of our study is a relatively small sample size of 14 subjects [15]. Future studies could include repeating part II of this study with a larger sample size. As well, future research could include addition of the lower dentition as part of the integration method or could focus on 4D capturing of the craniofacial complex, including dynamic movements in real time.

Figure 4.1: Trios vertical scan limit test on mannequin extra-oral facial scan

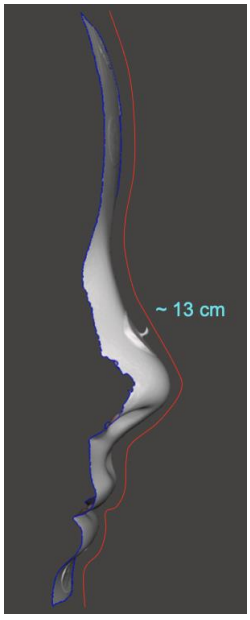

Chapter 5: Conclusions

The following conclusions can be drawn from the study:

1. The Bellus Arc7 facial scanner can produce 3D images with accuracy that is clinically acceptable for diagnosis, treatment planning and treatment outcome assessment.
2. Creation of a 3D virtual patient using the novel method of merging the bridge of nose and forehead scan taken on the Trios intraoral scanner with the Bellus Arc7 3D facial scan is feasible under static conditions with higher accuracy of the facial than the dental components.

Bibliography

[1] J. M. Plooij, T. J. J. Maal, P. Haers, W. A. Borstlap, A. M. Kuijpers-Jagtman, and S. J. Bergé, "Digital three-dimensional image fusion processes for planning and evaluating orthodontics and orthognathic surgery. A systematic review," *Int. J. Oral Maxillofac. Surg.*, vol. 40, no. 4, pp. 341–352, 2011, doi: 10.1016/j.ijom.2010.10.013.

[2] C. X. Nguyen, J. Nissanov, C. Öztürk, M. J. Nuveen, and O. C. Tuncay, "Three-dimensional imaging of the craniofacial complex: Nguyen et al. 3D imaging of craniofacial complex," *Clin. Orthod. Res.*, vol. 3, no. 1, pp. 46–50, Feb. 2000, doi: 10.1034/j.1600-0544.2000.030108.x.

[3] O. H. Karatas and E. Toy, "Three-dimensional imaging techniques: A literature review," *Eur. J. Dent.*, vol. 8, no. 1, pp. 132–140, Jan. 2014, doi: 10.4103/1305-7456.126269.

[4] J. Liu, C. Zhang, R. Cai, Y. Yao, Z. Zhao, and W. Liao, "Accuracy of 3-dimensional stereophotogrammetry: Comparison of the 3dMD and Bellus3D facial scanning systems with one another and with direct anthropometry," *Am. J. Orthod. Dentofacial Orthop.*, vol. 160, no. 6, pp. 862–871, Dec. 2021, doi: 10.1016/j.ajodo.2021.04.020.

[5] H. H. Lin, W. C. Chiang, L. J. Lo, S. Sheng-Pin Hsu, C. H. Wang, and S. Y. Wan, "Artifact-resistant superimposition of digital dental models and cone-beam computed tomography images," *J. Oral Maxillofac. Surg.*, vol. 71, no. 11, pp. 1933–1947, Nov. 2013, doi: 10.1016/j.joms.2013.06.199.

[6] C. Hong *et al.*, "Evaluation of the 3dMDface system as a tool for soft tissue analysis," *Orthod. Craniofac. Res.*, vol. 20, pp. 119–124, Jun. 2017, doi: 10.1111/ocr.12178.

[7] O. Erten and B. N. Yilmaz, "Three-Dimensional Imaging in Orthodontics," *Turk. J. Orthod.*, vol. 31, no. 3, pp. 86–94, Aug. 2018, doi: 10.5152/TurkJOrthod.2018.17041.

[8] D. Elmoutawakkil and N. Hacib, "Digital Workflow for Homemade Aligner," in *Dentistry*, vol. 9, F. Bourzgui, Ed. IntechOpen, 2022. doi: 10.5772/intechopen.100347.

[9] P. G. M. Knoops *et al.*, "Comparison of three-dimensional scanner systems for craniomaxillofacial imaging," *J. Plast. Reconstr. Aesthet. Surg.*, vol. 70, no. 4, pp. 441–449, Apr. 2017, doi: 10.1016/j.bjps.2016.12.015.

[10] G. Petrides, J. R. Clark, H. Low, N. Lovell, and T. J. Eviston, "Three-dimensional scanners for soft-tissue facial assessment in clinical practice," *J. Plast. Reconstr. Aesthet. Surg.*, vol. 74, no. 3, pp. 605–614, Mar. 2021, doi: 10.1016/j.bjps.2020.08.050.

[11] L. G. Farkas and C. K. Deutsch, "Anthropometric determination of craniofacial morphology," *Am. J. Med. Genet.*, vol. 65, no. 1, pp. 1–4, Oct. 1996, doi: 10.1002/ajmg.1320650102.

[12] T. Joda, U. Bragger, and G. Gallucci, "Systematic Literature Review of Digital Three-Dimensional Superimposition Techniques to Create Virtual Dental Patients," *Int. J. Oral Maxillofac. Implants*, vol. 30, no. 2, pp. 330–337, Mar. 2015, doi: 10.11607/jomi.3852.

[13] C. Mangano, F. Luongo, M. Migliario, C. Mortellaro, and F. G. Mangano, "Combining intraoral scans, cone beam computed tomography and face scans: The virtual patient," *J. Craniofac. Surg.*, vol. 29, no. 8, pp. 2241–2246, 2018, doi: 10.1097/SCS.0000000000004485.

[14] J. J. Wampfler and N. Gkantidis, "Superimposition of serial 3-dimensional facial photographs to assess changes over time: A systematic review," *Am. J. Orthod. Dentofacial Orthop.*, vol. 161, no. 2, pp. 182-197.e2, Feb. 2022, doi: 10.1016/j.ajodo.2021.06.017.

[15] F. Marradi, E. Staderini, M. A. Zimbalatti, A. Rossi, C. Grippaudo, and P. Gallenzi, "How to obtain an orthodontic virtual patient through superimposition of three-dimensional data: A systematic review," *Appl. Sci. Switz.*, vol. 10, no. 15, Aug. 2020, doi: 10.3390/APP10155354.
[16] H.-N. Mai and D.-H. Lee, "The Effect of Perioral Scan and Artificial Skin Markers on the Accuracy of Virtual Dentofacial Integration: Stereophotogrammetry Versus Smartphone Three-Dimensional Face-Scanning," *Int. J. Environ. Res. Public. Health*, vol. 18, no. 1, p. 229, Dec. 2020, doi: 10.3390/ijerph18010229.
[17] I.-D. Jeong, J.-J. Lee, J.-H. Jeon, J.-H. Kim, H.-Y. Kim, and W.-C. Kim, "Accuracy of complete-arch model using an intraoral video scanner: An in vitro study," *J. Prosthet. Dent.*, vol. 115, no. 6, pp. 755–759, Jun. 2016, doi: 10.1016/j.prosdent.2015.11.007.
[18] F. A. Rangel *et al.*, "Integration of digital dental casts in 3-dimensional facial photographs," *Am. J. Orthod. Dentofacial Orthop.*, vol. 134, no. 6, pp. 820–826, Dec. 2008, doi: 10.1016/j.ajodo.2007.11.026.
[19] M. G. Pérez-Giugovaz, S. H. Park, and M. Revilla-León, "Three-dimensional virtual representation by superimposing facial and intraoral digital scans with an additively manufactured intraoral scan body," *J. Prosthet. Dent.*, vol. 126, no. 4, pp. 459–463, Oct. 2021, doi: 10.1016/j.prosdent.2020.07.012.
[20] T. Joda and G. O. Gallucci, "The virtual patient in dental medicine," *Clin. Oral Implants Res.*, vol. 26, no. 6, pp. 725–726, Jun. 2015, doi: 10.1111/clr.12379.
[21] Y. S. N. Jayaratne, C. P. J. McGrath, and R. A. Zwahlen, "How Accurate Are the Fusion of Cone-Beam CT and 3-D Stereophotographic Images?," *PLoS ONE*, vol. 7, no. 11, Nov. 2012, doi: 10.1371/journal.pone.0049585.
[22] P. Zedníková Malá, V. Krajíček, and J. Velemínská, "How tight is the relationship between the skeletal and soft-tissue facial profile: A geometric morphometric analysis of the facial outline," *Forensic Sci. Int.*, vol. 292, pp. 212–223, Nov. 2018, doi: 10.1016/j.forsciint.2018.09.014.
[23] A. M. Ballo, C. T. Nguyen, and V. S. K. Lee, "Digital Workflow of Auricular Rehabilitation: A Technical Report Using an Intraoral Scanner," *J. Prosthodont.*, vol. 28, no. 5, pp. 596–600, Jun. 2019, doi: 10.1111/jopr.13057.
[24] T. K. Koo and M. Y. Li, "A Guideline of Selecting and Reporting Intraclass Correlation Coefficients for Reliability Research," *J. Chiropr. Med.*, vol. 15, no. 2, pp. 155–163, Jun. 2016, doi: 10.1016/j.jcm.2016.02.012.
[25] R. E. Donatelli and S.-J. Lee, "How to report reliability in orthodontic research: Part 1," *Am. J. Orthod. Dentofacial Orthop.*, vol. 144, no. 1, pp. 156–161, Jul. 2013, doi: 10.1016/j.ajodo.2013.03.014.
[26] D. Marques, R. Alves, R. Pinto, J. Caramês, H. Francisco, and J. Caramês, "Facial Scanner Accuracy with Different Superimposition Methods: An In Vivo Study," *Int. J. Prosthodont.*, vol. 34, no. 5, pp. 578–584, Sep. 2021, doi: 10.11607/ijp.7253.
[27] J. Y. Wong *et al.*, "Validity and Reliability of Craniofacial Anthropometric Measurement of 3D Digital Photogrammetric Images," *Cleft Palate. Craniofac. J.*, vol. 45, no. 3, pp. 232–239, May 2008, doi: 10.1597/06-175.
[28] S. C. Aung, R. C. K. Ngim, and S. T. Lee, "Evaluation of the laser scanner as a surface measuring tool and its accuracy compared with direct facial anthropometric measurements," *Br. J. Plast. Surg.*, vol. 48, no. 8, pp. 551–558, 1995, doi: 10.1016/0007-1226(95)90043-8.

[29] H. N. Mai, J. Kim, Y. H. Choi, and D. H. Lee, “Accuracy of portable face-scanning devices for obtaining three-dimensional face models: A systematic review and meta-analysis,” *Int. J. Environ. Res. Public. Health*, vol. 18, no. 1, pp. 1–15, Jan. 2021, doi: 10.3390/ijerph18010094.
[30] J. Winkler and N. Gkantidis, “Trueness and precision of intraoral scanners in the maxillary dental arch: an in vivo analysis,” *Sci. Rep.*, vol. 10, no. 1, p. 1172, Dec. 2020, doi: 10.1038/s41598-020-58075-7.
[31] M. H. J. Hollander *et al.*, “Reproducibility of 3D scanning in the periorbital region,” *Sci. Rep.*, vol. 11, no. 1, Dec. 2021, doi: 10.1038/s41598-021-83335-5.
[32] W. Piedra-Cascón, M. J. Meyer, M. M. Methani, and M. Revilla-León, “Accuracy (trueness and precision) of a dual-structured light facial scanner and interexaminer reliability,” *J. Prosthet. Dent.*, vol. 124, no. 5, pp. 567–574, Nov. 2020, doi: 10.1016/j.prosdent.2019.10.010.
[33] Z. Xiao, Z. Liu, and Y. Gu, “Integration of digital maxillary dental casts with 3D facial images in orthodontic patients:,” *Angle Orthod.*, vol. 90, no. 3, pp. 397–404, May 2020, doi: 10.2319/071619-473.1.